OPEN

Polymer Journal (2016) 48, 571–588

www.nature.com/pj

FOCUS REVIEW

Molecular design of photorefractive polymers

Naoto Tsutsumi

This review article describes the current state-of-the-art research on organic photorefractive polymer composites. A historical background on photorefractive materials is first introduced and is followed by a discussion on the opto-physical aspects and the mechanism of photorefractivity. The molecular design of photorefractive polymers and organic compounds is discussed, followed by a discussion on optical applications of the photorefractive polymers.
Polymer Journal (2016) **48,** 571–588; doi:10.1038/pj.2015.131; published online 27 January 2016

BACKGROUND

In this report, the molecular design of organic photorefractive (PR) polymers is reviewed. Organic PR polymers are materials that possess both electro-optical and photoconductive properties. Research on photoconductive polymers, whose pioneering polymer is poly(*N*-vinyl carbazole) (PVK, PVCz), began in the 1960s. From the 1980s, research on organic nonlinear optical (NLO) materials has been widely conducted in the fields of organic electro-optics and optical nonlinearity. From the 1990s, new technology using organic photorefractivity combined with photoconductive and electro-optical properties was introduced in the field of organic semiconducting materials,[1] and organic light-emitting diodes[2–6] and organic field-effect transistors[7] were also debuted in this field. At the same time, the interest of researchers also turned toward the development of organic photovoltaic cells and organic solar cells.[8–11] The transport of charge carriers through photoconductive manifolds is a common phenomenon found in PR, organic light-emitting diode or organic photovoltaic materials. Thus, the development of materials in each field is expected to merge together to trigger the development of novel materials.

The PR effect is a well-known phenomenon that is observed in materials in which refractive index modulation is induced by the space-charge field that results from the redistribution of positive and negative charge carriers separated through photo-excitation.[12] This phenomenon was first reported in inorganic crystals of lithium niobate ($LiNbO_3$) and lithium tantalate ($LiTaO_3$) and was observed through heterogeneous optically induced refractive indices in 1966.[13] Since then, the PR effect has extensively been investigated in many inorganic crystals, and theoretical approaches have been established to explain this phenomenon.[14]

In 1991,[1] the first study of PR polymers reported a low diffraction efficiency of 10^{-3} to 1% and a small optical gain of 0.33 cm^{-1}. In 1994,[15] a high diffraction efficiency of 86% (the remaining 14% was attributed to optical losses) and a large optical gain exceeding 200 cm^{-1} was reported in photoconductive PVK-based PR composites. Over the past two decades, many featured review articles[16–27] and book chapters[28–35] have been published, which have given us a technical understanding, and have provided researchers in the field with a direction for the development of relevant applications. The latest comprehensive review on PR polymer composites was reported in 2011,[26] and a review on its applications for holography was published in 2014.[27]

This review highlights the current state-of-the-art research on organic PR polymer composites with a specific focus on the response speeds (inverse of response time) of PR optical diffraction and amplification processes. PR phenomena and mechanisms are overviewed in the PR phenomena and mechanisms section. Molecular design of PR polymers section summarizes the molecular design of PR materials with an overview on the role of each component in the PR materials. The effects of molecular structure, especially the effects of molecular weight on PR properties, are discussed in the Effects of modifying molecular structures: molecular weight section. In the Effects of altering grating pitches section, the effects of altering grating pitch on PR properties are summarized. The correlation between photoconductivity and PR time responses are discussed in the Photoconductivity and response times section. PR response in a centrosymmetric environment section summarizes studies on asymmetric energy transfer in centrosymmetric media developed over the past two decades. Optical applications of organic PR polymer composites are summarized in the Optical applications section. The final section, Conclusions and future perspectives section, concludes this review and addresses future research directions and perspectives.

PR PHENOMENA AND MECHANISMS

The PR effect is a NLO effect based on the first-order electro-optic effect, also known as the Pockels effect. Pockels effect is well known as a nonlinear change in the refractive index of a noncentrosymmetric material that is induced by a DC field. In general, the PR effect appears in materials that are irradiated by coherent interference beams. In the bright region of an illuminated region, the charge carriers are separated via photo-excitation of photoconductive polymers and

Faculty of Materials Science and Engineering, Kyoto Institute of Technology, Kyoto, Japan
Correspondence: Professor N Tsutsumi, Faculty of Materials Science and Engineering, Kyoto Institute of Technology, 1 Hashigami-cho, Matsugasaki, Sakyo, Kyoto 606-8585, Japan.
E-mail: tsutsumi@kit.ac.jp
Received 16 September 2015; revised 23 November 2015; accepted 23 November 2015; published online 27 January 2016

sensitizers. Upon illumination, hole and electron charge carriers are separated under an applied electric field, and the hole carriers usually move through transport manifolds with assistance from the electric field and are captured by traps in dark regions. Space charge fields between electron charge carriers stay in the bright regions, and hole charge carriers are formed in the dark regions to induce changes in refractive indices via the Pockels effect. Resultant changes in refractive indices are periodically formed. A schematic diagram of the PR effect in materials is illustrated in Figure 1. Optical diffraction is measured from induced refractive index modulation. As shown in Figure 1, refractive index modulation shifts from the interference illumination pattern, which generates a unique PR optical amplification property as a result of asymmetric energy transfer.

By using the coupled wave theory developed by Kogelnik,[36] optical diffraction for p-polarized probe beam η is defined as

$$\eta = \sin^2\left[\frac{\pi d\Delta n\cos(\theta_B-\theta_A)}{\lambda\sqrt{\cos\theta_A\cos\theta_B}}\right] \quad (1)$$

where d is the sample thickness, λ is the laser wavelength, and θ_A and θ_B are the internal angles between the normal to the sample surface and the A and B beams, respectively. From this relationship, the refractive index modulation amplitude Δn of the PR composite can be evaluated.

Optical gain Γ is related to Δn through Equation (2),[37]

$$\Gamma = \frac{4\pi}{\lambda}(\hat{e}_1\cdot\hat{e}_2^*)\Delta n\sin\phi \quad (2)$$

where $\hat{e}_1$ and $\hat{e}_2$ are the polarization unit vectors of the two writing beams, and Φ is the phase shift between a refractive index modulation and an illumination pattern.

PR performance is generally evaluated using optical diffraction and optical amplification due to asymmetric energy transfer. The above diffraction efficiency η is a measure of optical diffraction, and optical gain Γ is a measure for optical amplification. In addition to these steady-state values, the response rates (inverse of response times) of these quantities are also important for evaluating PR dynamics. To evaluate PR dynamics, the time responses of these quantities can be

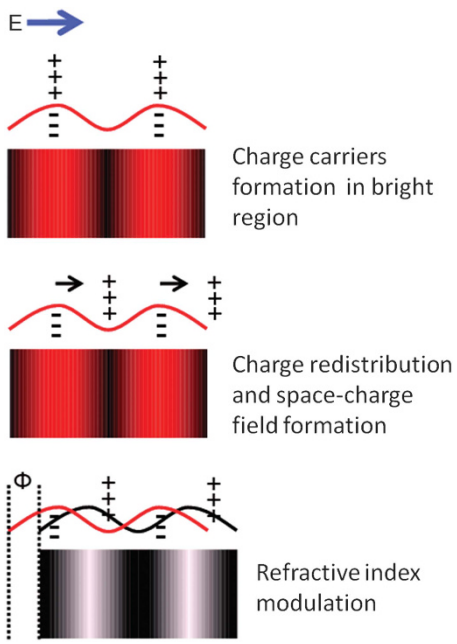

Figure 1 Schematic diagram of the photorefractive phenomenon.

evaluated using a stretched exponential function of Kohlrausch-Williams-Watts (KWW), as shown in Equations (3a) and (3b)[38]

$$\eta = \eta_0\left\{1-\exp\left[-\left(\frac{t}{\tau}\right)^{\beta}\right]\right\} \quad (3a)$$

or

$$\Gamma = \Gamma_0\left\{1-\exp\left[-\left(\frac{t}{\tau}\right)^{\beta}\right]\right\}, \quad (3b)$$

where t is time, η_0 is the steady-state diffraction efficiency, Γ_0 is the steady-state optical gain, τ is the grating build-up time, and β is the parameter related to the deviation from single exponential behavior ($0\leqslant\beta<1$). Bi-exponential fittings of Equations (4a) and (4b) are also widely used,[39]

$$\eta = \eta_0\left\{p\left[1-\exp\left(-\frac{t}{\tau_1}\right)\right]+(1-p)\left[1-\exp\left(-\frac{t}{\tau_2}\right)\right]\right\}^2 \quad (4a)$$

or

$$\Gamma = \Gamma_0\left\{p\left[1-\exp\left(-\frac{t}{\tau_1}\right)\right]+(1-p)\left[1-\exp\left(-\frac{t}{\tau_2}\right)\right]\right\}^2 \quad (4b)$$

where τ_1 is the fast component of response time, τ_2 is the slow component of response time, and p is the contribution of the fast component ($0<p<1$).

The average response time of a bi-exponential fitting is usually nearly equal to the KWW response time: $p\tau_1+(1-p)\tau_2\approx\tau$. We can compare these data with each response time. Diffraction efficiencies and optical gains are usually not affected by the intensity of the laser used for illumination, but the response times for these quantities are significantly affected by laser intensities.[40] Thus, a universal measure is required to characterize PR performance; sensitivity (S) defined as

$$S = \frac{\sqrt{\eta_{ext}}}{I\tau}$$

or

$$S = \frac{\sqrt{\eta_{ext}}}{I\tau L} \quad (5)$$

is used[27] where I is the total intensity of the writing laser beam and L is the thickness of the PR composite film. Here, η_{ext} is the external diffraction efficiency defined by

$$\eta_{ext} = \exp\left(-\frac{\alpha d}{\cos\theta_A}\right)\eta \quad (6)$$

where α is the absorption coefficient.

Typical PR quantities for different types of PR polymer composites in the literature are summarized in Table 1.[39,41–50] Usually, diffraction efficiencies and response times have electric field and wavelength dependencies. Furthermore, glass transition temperatures (T_g) also affect these quantities. Therefore, as noted by a previous study,[49] a true comparison is difficult because of the different experimental conditions, such as film thicknesses, wavelengths employed, the applied electric fields and the T_gs of the corresponding PR composites.

The Kukhtarev[14] model predicts the space-charge field E_{SC}:

$$|E_{SC}|\approx E_q\left(\frac{E_D^2+E_0^2}{E_0^2+(E_q+E_D)^2}\right)^{1/2} \quad (7)$$

where E_D is the diffusion field ($E_D=K_GkT/e$; K_G is the grating wave vector, k is Boltzmann constant, T is the absolute temperature and e is the electronic charge). The Kukhtarev[14] model also predicts the phase

shift Φ between refractive index modulation and an illumination pattern:

$$\tan \Phi = \left[\frac{E_D}{E_0}\left(1 + \frac{E_D}{E_q} + \frac{E_0^2}{E_D E_q}\right)\right] \quad (8)$$

The trap-limited space-charge field E_q can be related to the number of density of traps, N_T, as follows:

$$E_q = \frac{eN_T}{\varepsilon_r \varepsilon_0 K_G} \quad (9)$$

Table 1 Typical photorefractive data for different types of photorefractive composites reported in the literature

Material composition (wt%)	*λ (nm)*	*I (W cm^{-2})*	*E (V μm^{-1})*	*η/η$_{ext}$ (%)*	*τ/τ^{-1}(ms/s^{-1})*	*S (cm^2 J^{-1})*	*Ref.*
PTAA/PDCST/TAA/PCBM/Alq3 (43.5/35/20/0.5/1)	532	0.535	60	83	0.86/1162	437	41
PTAA/PDCST/TAA/PCBM (44.5/35/20/0.5)	532	0.427	45	47.0/1.6	10.2/98	29	42
PDAA/7-DCST/BBP/PCBM (55/40/4/1)	532	0.172	25	33	267/3.3	13	43
PVK/7-DCST/ECZ/TNF (44/35/20/1)	532	0.17	45	91	230/4	11	44
PTPA-*g*-PEA/DEADCST/TNF (90/9/1)	632.8	0.12	50	2.8	8/125	158	45
PATPD/7-DCST/ECZ/C_{60} (49.5/35/15/0.5)	632.8	1	55	85	8/125	104	46
PTAA/PDCST/TAA/PCBM (44.5/35/20/0.5)	632.8	1.5	45	16.6/10.3	5/200	43	42
Poly-TPD/P-IP-DC/BBP/PCBM (54/30/15/1)	632.8	0.06	30	67	334/2.9	38	47
PTAA/7-DCST/ECZ/PCBM (44/35/20/1)	632.8	1.5	20	6.4/5.1	11.3/88	13	39
P-THEA/DEANST (70/30)	632.8	0.13	50	5.4	220/4.5	7	48
TPD-PPV/AZO/DPP/PCBM (56/30/13/1)	830	0.64	60	1	8/125	19	49

Abbreviations: AZO, azo dyes; BBP, benzylbutylphthalate; DCST, aminodicyanostyrene; DEANST, 4-(N,N-diethylamino)-β-nitrostyrene; DEADCST, 4-N,N-diethylamino-β,β-dicyanostyrene; DPP, diphenyl phthalate; ECZ, *N*-ethylcarbazole; PATPD, polyacrylic TPD; PCBM, 6,6-phenyl-C61-butyric acid methyl ester; PDAA, poly(4-diphenylamino)benzyl acrylate; PDCST, 4-piperidinobenzylidene-malononitrile; PTPA-g-PEA, polytriphenylamine-graft-poly(ethyl acrylate); P-IP-DC, 2-{3-[(E)-2-(piperidino)-1-ethenyl]-5,5-dimethyl-2-cyclohexenylidene}-malononitrile; P-THEA, polymer containing a thioxanthene unit; PTAA, poly(bis(4-phenyl)(2,4,6-trimethylphenyl)-amine); TNF, 2,4,7-trinitrofluorenone; TPD, tetraphenyldiaminophenyl; TAA, (2,4,6-trimethylphenyl)-diphenylamine; TPD-PPV, Poly (arylene vinylene) copolymer.

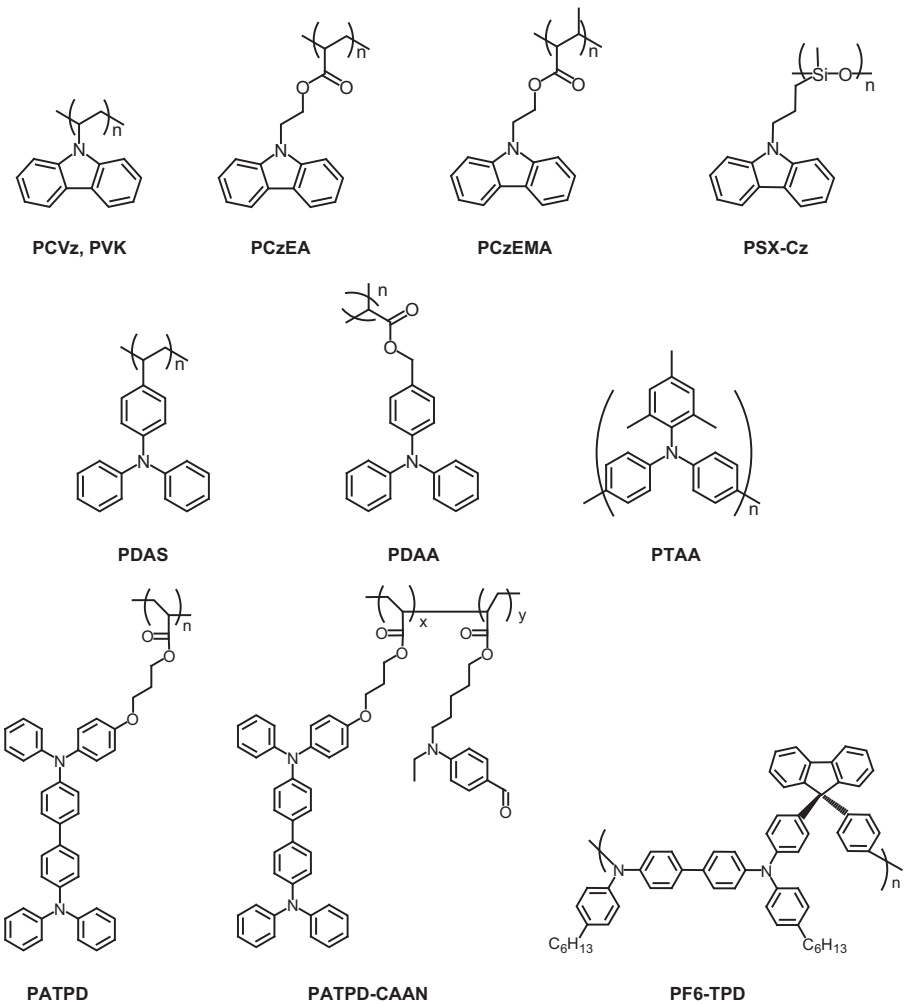

Figure 2 Structural formulae of photoconductive polymers and molecular glasses for photorefractive composites.

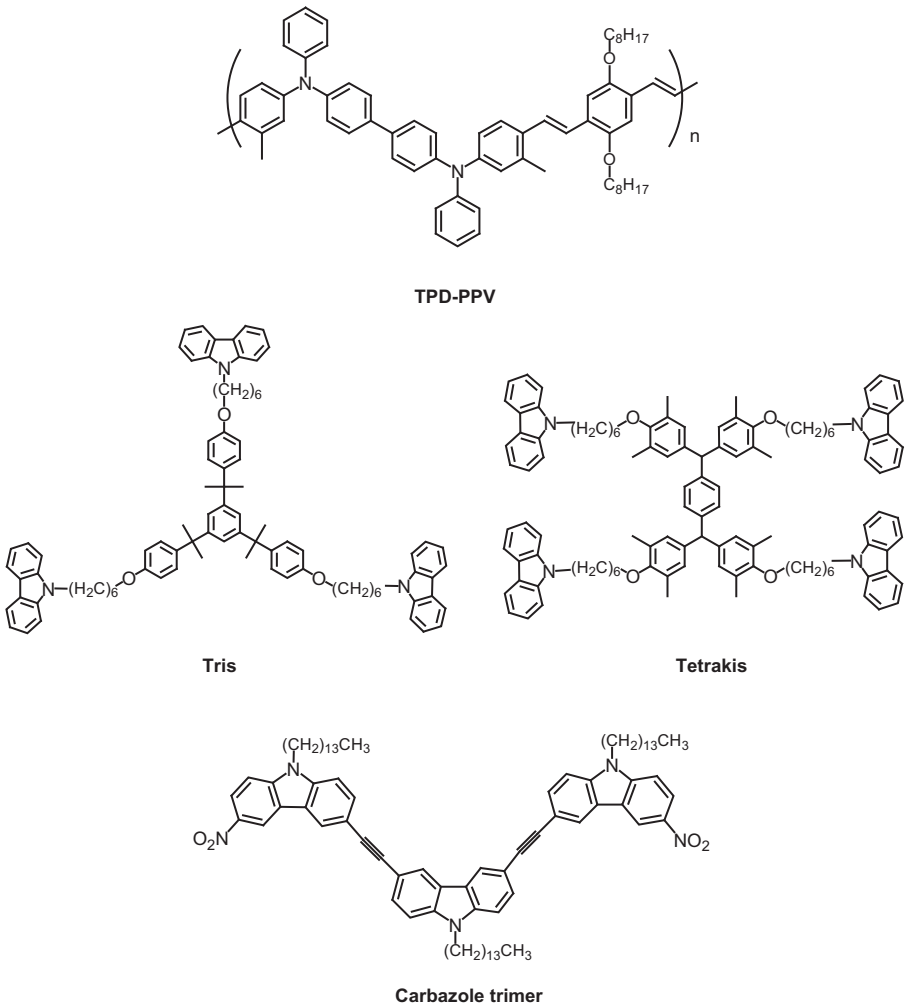

Figure 2 Continued.

where ε_r is the dielectric constant, and ε_0 is the permittivity in vacuum.

MOLECULAR DESIGN OF PR POLYMERS

As mentioned above, photoconductive properties and second-order optical nonlinearity are required to fabricate PR polymers. PR polymers basically consist of photoconductive polymers, optical sensitizers, NLO chromophores and plasticizers.

Photoconductive polymers

The structural formulae of photoconductive polymers and molecular glasses are summarized in Figure 2.

Carbazole-based polymers and molecular glasses. PVK (or PVCz) is a well-known photoconductive polymer. PVK has extensively been investigated as an organic photoconductor for use in copy machines and laser (recently light-emitting diode) printers. PVK, a pioneer photoconductive polymer, has also extensively been studied for use as PR host polymers. Many studies on the PR performance of materials based on PVK have been reported over the past two decades. Zhang *et al.*[50] reported the PR performance of a PVK-based polymer composite with DEANST as a NLO dye and fullerene as a sensitizer. An almost complete diffraction efficiency of 86% and optical gain of more than 200 cm^{-1} were reported in a PVK/2,5-dimethyl-4-(nitrophenylazo)anisole (DMNPAA)/*N*-ethylcarbazole (ECZ)/2,4,7-trinitrofluorenone (TNF) PR system.[15] A response time in the order of milliseconds for two beam-coupling measurements was first reported in PVK/7-aminodicyanostyrene (7-DCST), 4-piperidinobenzylidene-malononitrile (PDCST), 2-[4-bis(2-methoxyethyl)amino]benzylidene]malononitrile (AODCST) or 2-[[4-(diethylamino)-2-(trifluoromethyl)phenyl]methylidene]propanedinitrile (TDDCST)/benzylbutylphthalate (BBP)/C_{60} PR systems at an extremely high electric field of 100 V μm^{-1} and under an illumination of 1 W cm^{-2}.[38] A fast response time of 20 ms was observed for a PVK PR composite.[51] A polyacrylate PR composite with carbazole as a pendant group was designed, and its PR performance was found to be almost identical to a PVK-based PR composite.[52] A PR molecular glass of a multifunctional conjugated carbazole trimer (Figure 2) was also designed, and an optical gain of 35.0 cm^{-1} (net gain of 26.8 cm^{-1}) was recorded under $E = 33$ V μm^{-1} at 532 nm.[53] PR molecular glasses of star-shaped molecules end-caped with carbazole moieties (Tris and Tetrakis in Figure 2) were designed; in transmission mode, diffraction efficiencies in the range of 40–60% and optical gains in the range of 50–75 cm^{-1} were observed,[54] and in reflection mode, a net optical gain of 33 cm^{-1} was obtained at 57.7 V μm^{-1} for a Tetrakis composite.[55]

Recently, enhanced PR performances of poly(methyl-3-(9-carbazolyl)propylsiloxane) (PSX-Cz)-based composites through surface plasmon effects of gold nanoparticles were reported.[56] Surface

plasmon resonance of gold nanoparticles enhanced their photoconductivity and PR response. Off-resonance photosensitized PR properties were investigated for PVK/AODCST/ECZ composite with quantum-dot PbS nanocrystals,[57] and a large optical gain of 211 cm^{-1} was obtained.

Triphenylamine-based polymers. Extensive studies described above on PVK-based PR polymer composites have been performed over the past two decades. However, the average response time for optical diffraction and optical amplification in PVK-based PR composites has been limited to a couple of tens or hundreds of milliseconds in order response times under moderate electric fields. This is ascribed to the low hole mobility, which is on the order of 10^{-7}–10^{-6} $cm^2\ V^{-1}\ s^{-1}$, for PVK pristine polymers. An ionization potential (I_p) of 5.9 eV was observed for PVK (Ionization potential of PVK is measured by photoelectron yield spectroscopy in air using an AC-3 spectrometer (Riken Keiki)).

Similar to the PVK- and Cz-based polymers, triphenylamine (TPA) and tetraphenyldiaminophenyl (TPA dimer, TPD) moieties can also be used as hole transport manifolds. An ionization potential (I_p) of TPA was reported to range from 5.30[58] to 5.70 eV (Ionization potential of TPA is measured by photoelectron yield spectroscopy in air using an AC-3 spectrometer (Riken Keiki)), which is lower than that of PVK. Thus, fast hole mobility was expected. A polymer with a TPD moiety was shown to have hole mobility in the range of 10^{-5}–10^{-4} $cm^2\ V^{-1}\ s^{-1}$.[59] PR responses and applications for the polyacrylic TPD (PATPD)-based PR composites have been extensively investigated.[46] The responses and applications of a PF6-TPD PR composite have also been investigated.[60]

Another type of TPA-based PR polymer has also been investigated. The PR response of a vinyl polymer of a TPA moiety directly attached to the backbone, poly(4-diphenylamino)styrene (PDAS), was compared with that of a PVK-based corresponding polymer.[61] PDAS had a hole mobility in the range of 10^{-4}–10^{-3} $cm^2\ V^{-1}\ s^{-1}$. PDAS/7-DCST/diphenyl phthalate (DPP)/TNF showed a decreased growth time of 0.4 s for optical diffraction, which was faster than that of PVK/7-DCST/DPP/TNF and had a growth time of 1.2 s.[61] The PDAS composite also had a faster rise time and a larger intensity for photocurrent compared to the PVK composite.[61] By changing the sensitizer from TNF to PCBM, the NLO dye from 7-DCST to FDCST, and the plasticizer from DPP to ECZ, the diffraction efficiency of PDAS/2-(4-(azepan-1-yl)-2-fluorobenzylidene (FDCST)/ECZ/6,6-phenyl-C61-butyric acid methyl ester (PCBM) improved by 35% and had a response time of 39 ms at 45 V μm^{-1}, allowing a demonstration of real-time recording and simultaneously displaying a two-dimensional (2D) holographic images.[62] Furthermore, these changes improved the optical diffraction by up to 90% using the same composites.[63]

The development of polyacrylic TPA-based PR polymers has also been reported.[43,64] A high diffraction efficiency of $>80\%$ at moderate electric field of 40 V μm^{-1} was achieved for a poly(4-diphenylamino) benzyl acrylate (PDAA)-based PR polymer, PDAA/7-DCST/BBP/PCBM.[43,64] The authors also demonstrated a clear and updatable 2D hologram recording, and simultaneously reconstructed it in real time at a low electric field of 25 V μm^{-1}.[43]

Another type of PR polymer with TPA in the main chain is a graft copolymer, consisting of a poly(triphenylamine) backbone, poly(ethyl acrylate) branches[45] and a methyl-substituted poly(triarylamine), also known as poly(bis(4-phenyl)(2,4,6-trimethylphenyl)-amine) (PTAA).[39,41,42] PTAA features large hole mobility in the range of 10^{-3}–10^{-2} $cm^2\ V^{-1}\ s^{-1}$. However, due to this high hole mobility, it has a large amount of dark conductivity, which easily leads to dielectric breakdown and limits the applying voltage. This dielectric breakdown is caused by the narrow width between the Fermi level (E_F) of indium tin oxide (ITO), −4.8 eV, and the highest occupied molecular orbital (E_{HOMO}) of PTAA, −5.2 eV. Kinashi *et al.* successfully modified E_F by adding a self-assembled monolayer onto an ITO electrode. The resulting E_F was −4.3 eV, which significantly suppressed the dark current, as shown in Figure 3.[39] The PR composites of PTAA, 7-DCST, ECZ and PCBM gave rise to a diffraction efficiency as low as a few percent with a response time of 11.3 ms under an applied electric field of 25 V μm^{-1} at 632. 8 nm. Modification of the NLO chromophore from 7-DCST to PDCST, and altering the plasticizer from ECZ to TAA achieved a diffraction efficiency of 16% with a response time of 5 ms, resulting in a sensitivity of 43 $cm^2\ J^{-1}$ under an applied electric field of 45 V μm^{-1} at 632.8 nm.[42] Further improvements in the response time (860 μs), the diffraction efficiency (83%) and sensitivity (437 $cm^2\ J^{-1}$) were achieved by adding Alq_3 as a second sensitizer.[41] The added Alq_3 coordinated with the charge transfer (CT) complex between PTAA and significantly suppressed the excess photocurrent, which played a significant role in achieving high PR performances. Rapid cycling of the PR responses at 100 Hz was performed. Figure 4 shows the asymmetric energy transfer signals when a rectangular field of 60 V μm^{-1} was externally applied at 100 Hz; a response time of 350 μs and decay time of 200 μs were observed.

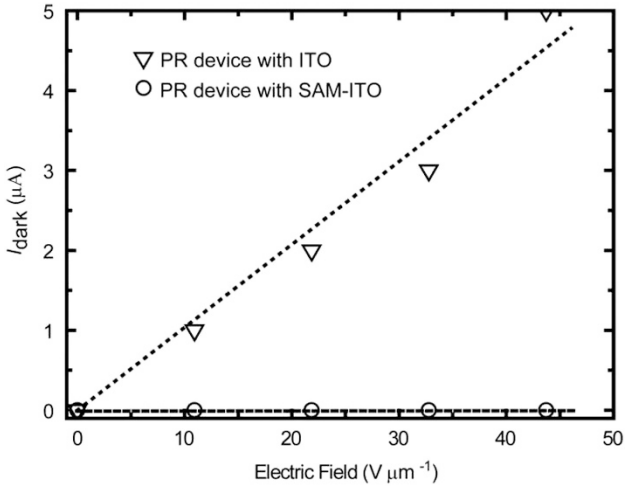

Figure 3 Plots of dark current as a function of an electric field with and without a self-assembled monolayer (SAM) interlayer on ITO. Reproduced from Kinashi *et al.*[39] with permission from Elsevier.

Sensitizers

Sensitizers are the important component in PR polymer composites because they strongly assist the generation of charge carriers through photo-excitation. Almost all photoconductive polymer materials are p-type hole-conducting materials; thus, most sensitizers are n-type electron acceptors, as shown in Figure 5. The charge carriers are, in some cases, generated through light absorption by a sensitizer and are also generated through photo-excitation of the CT complex between a p-type host photoconductor and an n-type sensitizer. Charge carrier photogeneration via a CT complex between PVK and TNF has extensively been studied in the field of organic photoconductor in the 1960s and 1970s.[65,66] In the early stages of studies on organic photorefractivity, fullerene (C_{60}) was used as a useful n-type sensitizer.[67] Doping of only 0.2 wt% of C_{60} drastically increased DC photoconductivity, the grating growth rate, and the diffraction

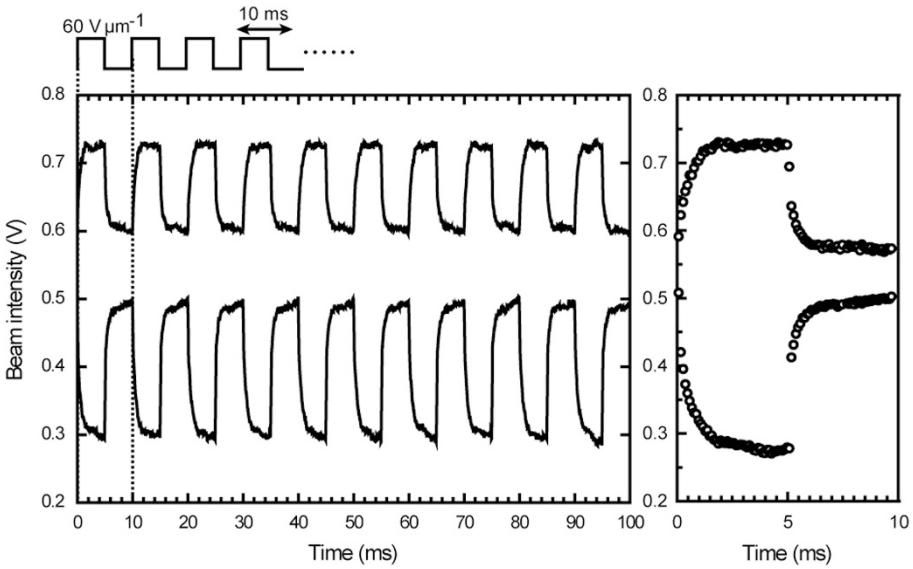

Figure 4 Left: sequence response of the optical gain for a PTAA PR composite upon applying a rectangular field at a frequency of 100 Hz. Right: one cycle response; a response time of 350 μs and a decay time of 200 μs. Reproduced from Tsutsumi *et al.*[41] with permission from the Optical Society of America.

efficiency by a factor of 20.[67] Sensitization by C_{60} led to a small increase in the carrier generation efficiency and a large increase in optical absorption of photons at an operating wavelength of 647 nm.[67] Sensitization by an ionic dye, thiapyrylium, was investigated in PVK PR composites.[68,69] Thiapyrylium dye is known to be formed as an aggregate with bisphenol A polycarbonate.[70,71] The aggregates changed the absorption peak from 590 to 700 nm, which placed the PR potential in the near-infrared region.[68,69] By using a 703-nm laser, a diffraction efficiency of 2% and optical gain of 7 cm^{-1} were observed.[68,69] The J-aggregate of the carbocyanine dye shifted the absorption peak from 570 (for non-aggregate) to 670 nm, and the polyimide sensitized by the J-aggregate of the carbocyanine dye gave rise to a large optical gain of 218 cm^{-1} (net gain of 143 cm^{-1}) with a 20 ms response.[72] The optical gain and response time of the PVK PR composite sensitized with a monolithic compound of TNF—C_{60} was compared with that sensitized with C_{60}.[73,74] The response time was faster but the optical gain was reduced.[74] The PR performance of PVK sensitized with quinone derivatives, including 2,3-dichloro-5,6-dicyano-*p*-benzoquinone (DDQ), 2,3,5,6-tetrachloro-*p*-benzoquinone (chloranil), 2,5-dichloro-*p*-benzoquinone (Cl_2Q), p-benzoquinone (BQ), 2,6-dimethyl-*p*-benzoquinone (MQ) and 1,2,4,5-tetracyanobenzene (TCNB), was compared with that sensitized with TNF.[75] In the series of quinones, a larger photocurrent resulted in a larger number density of traps and faster response rate.[75] The following PR performance of PVK sensitized with phthalocyanines was reported: high diffraction efficiency of 91%, an optical gain as large as 350 cm^{-1} and a response time of 100 ms.[76] The most remarkable observation was that a very small amount of a sensitizer (0.06×10^{-6} mmol mg^{-1}) was needed to give high performance, which suppressed the absorption loss and aggregation.[76] A series of near-infrared-sensitive PR composites based on PF6-TPD sensitized by fullerene derivatives was reported. When the reduction potential of fullerene derivative was lowered by 400 mV, the response time was found to be faster by one order of magnitude; other physical parameters remained identical.[60] The PR performance of a PVK-based composite sensitized by graphene was presented. No improvements in PR performance were observed due to the considerable amount of light scattering in the medium.[77] The PR performances of a graphene-sensitized PATPD PR composite were compared with that sensitized by a conventional fullerene derivative of PCBM. The addition of graphene laminates to a PR composite gave a threefold enhancement in the space-charge field build-up time.[78] By adding second electron traps consisting of tris(8-hydroxyquinoline) aluminum (Alq_3), a larger optical gain, higher diffraction efficiency and faster response time were observed at lower voltages for a PATPD-based PR composite with PCBM. Toughness against dielectric breakdown was also improved; investigations on the grating dynamics revealed the presence of competing gratings, and a bipolar charge transport model was found.[79] Tsutsumi *et al.* also investigated the effect of Alq_3 on the PR performance of a PTAA-based PR composite with PCBM. A small amount of Alq_3 significantly improved the toughness of the material against dielectric breakdown, which led to a faster response time in the order of hundreds of microseconds.[41] The PR performances of perylene bisimide (PBI) and a dimer of PBI (DiPBI)-sensitized PVK PR composites were compared with that sensitized with PCBM. Photoconductivity was increased by a factor of 120 and 32 for the PBI and DiPBI-sensitized samples, respectively, and a 1/4 amount of the DiPBI-sensitized PVK doubled the optical gain and increased the PR speed by 39 times compared to a PVK PR composite synthesized with PCBM.[80] The PR performance of the PBI-sensitized PDAA composite was investigated. PDAA with small amount of PBI (0.1 wt%) effectively formed the CT complex, which enhanced PR performance.[81]

NLO dyes

The photoconductors and sensitizers discussed above were used to produce the charge carriers (holes and electrons) upon the interference of light illumination under an external electric field. Positive charge carriers (hole) separated in the bright region commonly transport through hole transport manifolds and are trapped in dark regions of PR matrices. Redistribution of the charge carriers (holes and electrons) form space-charge field modulation with assistance of the external electric field in the PR matrix. The primary role of a NLO chromophore is to provide refractive index modulation through space-charge modulation. Numerous efforts have been made during 1980s and 1990s to develop a new class of NLO chromophores based on π-conjugated molecules for optimizing the optical nonlinearity

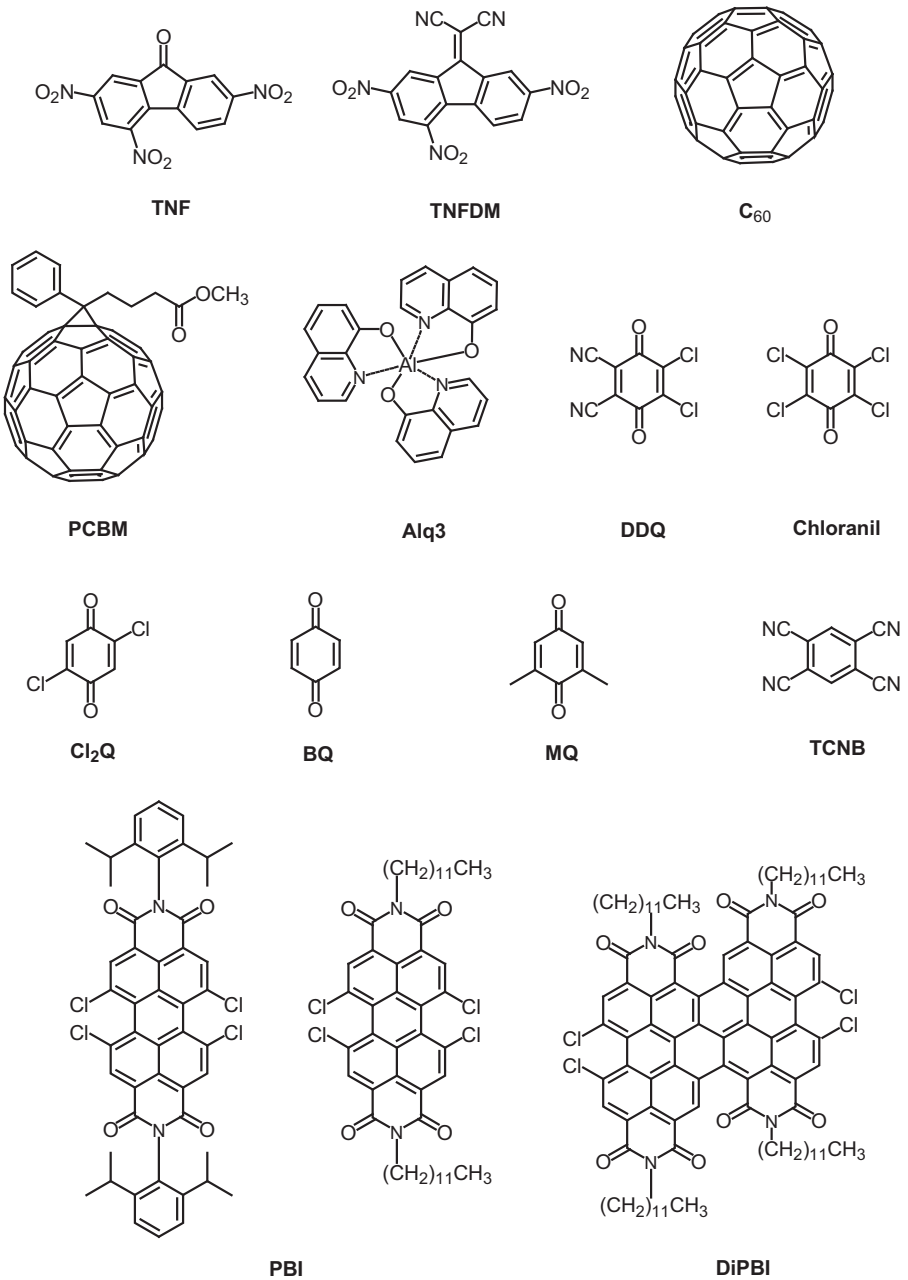

Figure 5 Structural formulae of the sensitizers used to generate photorefractive composites.

of electro-optic polymers.[82] In such cases, large second-order polarizability (first hyperpolarizability), β, and the dipole moment of the ground state, μ, were found to be important parameters for the development of larger second-order optical nonlinearity. In this case, a figure of merit (FOM) was defined as

$$\mathrm{FOM} = \frac{\mu\beta}{M} \tag{10}$$

where M is the molecular weight, μ is the ground-state dipole moment and β is the first hyperpolarizability (second-order polarizability). The π-conjugated molecules were end-capped with an electron-donating substituent group and an electron-accepting substituent group to enhance the larger second-order optical nonlinearity. When the photorefractivity of the organic PR polymers is attributed solely to the Pockels effect, like inorganic PR crystals such as $LiNbO_3$, larger second-order optical nonlinearity of the NLO chromophores become a target for developing better PR properties. This approach is valid for PR polymers with high T_gs. However, in the early stages of the invention of PR polymers, the photorefractivity of low T_g matrices was found to be enhanced by the birefringence effect due to the orientation of NLO chromophores.[83] The PR refractive index modulation was determined to originate from the electro-optic effect (Pockels effect) and the birefringence due to polarization anisotropy of the NLO chromophores. Thus, instead of using FOM in Equation (10), which uses the linear and NLO polarizabilities of NLO chromophores, another FOM of NLO chromophores was introduced and was

defined as[84]

$$\mathrm{FOM} = \mathrm{FOM_{BR}} + \mathrm{FOM_{EO}} = \frac{1}{M}\left(\frac{2\mu^2\Delta\alpha}{kT} + 9\mu\beta\right) \tag{11}$$

where $\Delta\alpha$ is the polarizability anisotropy, k is Boltzmann constant and T is the temperature.

Linear and nonlinear polarizabilities are simply calculated using a sum-over-states (SOS) method:[85]

$$\alpha = 2\frac{\mu_{ag}^2}{E_{ge}} = 2\frac{\mu_{ag}^2\lambda_{ag}}{hc_0} \tag{12}$$

$$\beta = 6\frac{\mu_{ag}^2\Delta\mu}{E_{ge}^2} = 6\frac{\mu_{ag}^2\Delta\mu\lambda_{ag}^2}{(hc_0)^2} \tag{13}$$

where μ_{ag} is the transition moment, $\Delta\mu$ is the difference of the dipole moments between the first excited and ground states ($\Delta\mu = \mu_e - \mu_g$, μ_e: the dipole moment in the first excited state, μ_g: the dipole moment in the ground state), E_{ge} is the band gap, λ_{ag} is the absorption maximum, h is Planck's constant and c_0 is the speed of light in a vacuum. In one-dimensional NLO chromophores, the tensor component of linear polarization in the dimension of the molecular axis is much larger than perpendicular components, and thus $\Delta\alpha \approx \alpha$ is satisfied. Experimental transition moments are calculated through integration of the absorption spectrum of the corresponding NLO chromophores. The dipole moment in the ground state and the difference of the dipole moments are calculated using electro-optical absorption measurements.[86]

Polarizability anisotropy $\Delta\alpha$, the ground-state dipole moment μ and the first hyperpolarizability β are significantly affected by structural modifications due to changes in the electron-donating and -accepting substituent groups. The two terms of FOM of the NLO chromophores with various π-conjugated structures with different electron-donating and -accepting substituent groups were individually evaluated as a function of the resonance parameter c^2 for two basic resonance states of push-pull chromophores, a neutral polyene limit (D–A, $c^2 = 0$), cyanine limit with $c^2 = 0.5$, zwitterionic limit (betaine type, D^+–A^-, $c^2 = 1$)[26,86,87] and as a function of π-bond-order alternations (BOAs).[27,88,89]

For π-conjugated molecules with single-double bond series, bond-length alternation (BLA) is defined in terms of the difference between the average lengths of single bonds and that of double bonds, which is significantly related to the optimized geometries.[85,90] BOA is defined as the difference between the average π-bond orders of the same two sets of bonds.[85,90] BLAs and BOAs are commonly found to have the following values: BLA = 0.1 Å and BOA = − 0.65 in neutral polyene limits; BLA = 0 Å and BOA = 0 in cyanine limits; and BLA = − 0.1 Å and BOA = 0.65 in zwitterionic limits.

$$\mu_{ag} = c\left(1 - c^2\right)^{1/2}\Delta \tag{14}$$

$$\Delta\mu = \left(1 - 2c^2\right)\Delta \tag{15}$$

$$\mu_g = c^2\Delta \tag{16}$$

In the above equations, Δ is the difference between the dipole moments of the neutral and the zwitterionic states, which are equal to the maximum change of the dipole upon excitation in a given system.[84] Equations (11)–(15) give Equation (17):[86]

$$c^2 = \frac{1}{2}\left[1 - \frac{\Delta\mu}{\left(4\mu_{ag}^2 + \Delta\mu^2\right)^{1/2}}\right] \tag{17}$$

Commonly used PR NLO molecules are summarized in Figure 6. Electro-optical quantities for various NLO chromophores are listed in Table 2. The value of FOM is plotted as a function of the resonance parameter c^2 for the corresponding NLO chromophores in Figure 7. The solid curve is calculated using Equation (11) with Equations (12)–(15). The same types of plots were reported by Würthner's group.[86,87] Kippelen *et al.*[88] also plotted the two terms of FOM and FOM as a function of BOA. The product of $\mu\beta$ was shown to have two extrema with a positive maximum (at $0 < c^2 < 0.5$, $-0.65 < \mathrm{BOA} < 0$), a negative maximum (at $0.5 < c^2 < 1$, $0 < \mathrm{BOA} < 0.65$) and zero at the cyanine limit ($c^2 = 0.5$, BOA = 0). Polarizability was found to have a maximum at the cyanine limit ($c^2 = 0.5$, BOA = 0). As listed in Table 2, the first term, $\mathrm{FOM_{BR}}$, due to the birefringence was more than ten times larger than the second term, $\mathrm{FOM_{EO}}$, due to the electro-optic effect. Thus, it was concluded that the polarization anisotropy of NLO chromophores due to the birefringence is usually dominant for the refractive index modulation. Namely, the contribution of the hyperpolarizability term due to the electro-optic effect (Pockels effect) was far outweighed by the contribution of the linear polarization term due to the birefringence of the NLO molecule by the space-charge field (molecular orientation enhancement).[26,27,86–89]

Beyond the cyanine limit ($c^2 > 0.5$, BOA > 0), some problems have been noted:[26,87] high-melting crystalline solids are generated, which lead to difficulties of dissolving the materials in rather non-polar polymeric matrices. Then, the molecular design around cyanine limits offers better NLO chromophores for enhanced PR performance.

Plasticizers

As discussed in NLO dyes section, the orientation of NLO chromophores plays an important role for PR polymers (orientational enhancement of the PR effect[83]); thus, the T_g of a PR polymer matrix should significantly affect PR properties. Plasticizers are commonly used to control the T_gs of PR polymers. Figure 8 summarizes the commonly used plasticizers. In PR polymers, photoconductive plasticizers such as ECZ,[15,39,44,62,63] carbazoylethylpropionate (CzEPA),[44,52,91] TPA,[62,63] 2,4,6-trimethylphenyl-diphenylamine (TAA)[41,42] and (4-(diphenylamino)phenyl)methanol (TPAOH)[64] have been commonly used. Photoconductive plasticizers with long alkyl chains, such as 9-(2-ethylhexyl)carbazole (EHCz),[92] have also been used. Other common plasticizers, such as BBP,[43,52,92–94] tricresyl phosphate (TCP),[55,93,94] DPP[52,93,94] and dicyclohexyl phthalate (DCP),[93,94] are often used.

ECZ, CzEPA and EHCz are carbazole derivatives, and these compounds are used with PVK and PATPD. EHCz is used as a liquid plasticizer. TPA is used with PDAS. TAA is used with PTAA. TPAOH is used with PDAA. Common plasticizers can be used with either of the polymers.

Fully functionalized organic PR materials

PR polymers are based on p-type photoconductive host polymers mixed with a NLO dye, a small amount of an n-type sensitizer, and a plasticizer. However, the polymer mixtures sometimes suffer from phase separations during long-term use. To avoid this inconvenience, fully functionalized, multifunctional or monolithic-type PR polymers

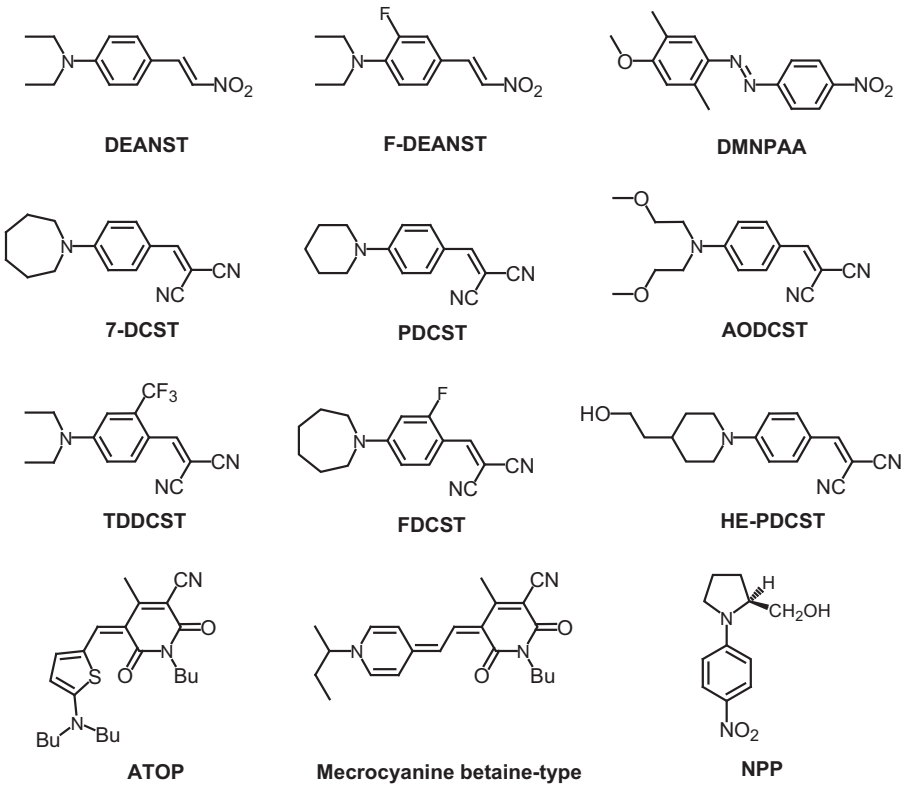

Figure 6 Structural formulae of NLO chromophores used to generate photorefractive composites.

Table 2 Electro-optical quantities for NLO chromophores and FOM values calculated by Equation (11)

NLO chromophore	c^2	μ_g (10^{-30} C m)	$\Delta\alpha$ (10^{-40} C m^2 V^{-1})	β (10^{-50} C m^3 V^{-2})	*M* (g mol^{-1})	FOM_{BR} (10^{-74} C^2 m^4 V^{-2} kg^{-1} mol)	FOM_{EO} (10^{-76} C^2 m^4 V^{-2} kg^{-1} mol)
F-DEANST[a]	0.12	21	22	78	238	0.197	6.19
DMNPAA[a]	0.16	21	22	56	269	0.174	3.93
PDCST[b]	0.22	29	25	52	237	0.429	5.73
ATOP[a]	0.45	47	55	27	427	1.37	2.67
Betaine type[a]	0.58	54	66	−61	361	2.58	−8.21

Abbreviations: ATOP, 1-alkyl-5-[2-(5-dialkylaminothienyl)methylene]-4-alkyl-[2,6-dioxo-1,2,5,6-tetrahydropyridine]-3-carbonitrile; DMNPAA, 2,5-dimethyl-4-(nitrophenylazo)anisole; FOM, figure of merit; F-DEANST, 3-fluoro-4-N,N-diethylamino-β-nitrostyrene; NLO, nonlinear optical; PDCST, 4-piperidinobenzylidene-malononitrile.
[a]Electro-optical data are taken from Würthner *et al.*[87]
[b]Electro-optical data are taken from Wortmann *et al.*[134]

and molecular glasses have been designed. Irrespective of the usefulness of these systems, the complexity of their syntheses and the reduction in the variations of their molecular design have limited the progress of research. Among these materials, monolithic PR polymers have been incorporated with photoconductive and nonlinear moieties into a single backbone as a solution for preventing such issues. In 2000, a review article was published discussing the progress of this research.[21]

Fully functionalized polymers. PR polymethacrylates functionalized with carbazole moieties and three types of NLO moieties are shown in Figure 9. A diffraction efficiency of 60% and an optical gain of 57 cm^{-1} were observed for the functionalized polymer having R3 NLO moiety with 1 wt% (2,4,7-trinitro-9-fluorenylidene)malononitrile (TNFDM) under $E = 58$ V μm^{-1} at 780 nm.[95] The PR performance of a series of PR polymethacrylates containing carbazoles and Disperse Red dye moieties was investigated at 780 nm. An optical gain coefficient of 140 cm^{-1} was measured with incorporation of a TNFDM sensitizer.[96] Low-T_g PR polyacrylates with carbazole and NLO moieties as pendant groups were designed. For these polymers, an optical gain coefficient of 122 cm^{-1} was obtained using 2 wt% of a TNF sensitizer at $E = 85$ V μm^{-1}.[97] Monolithic methacrylate polymers containing carbazole and dicyano-aminostyrene moieties through spacers (Figure 10) were synthesized using an analogous polymerization reaction. However, this led to an undesired side reaction that formed anhydride groups in the polymer backbone. Despite the presence of this undesired side reaction, the resulting monolithic polymer showed long-term stability.[98]

PR polysilanes functionalized with *N*-methyl-*p*-nitroaniline, as shown in Figure 11, were designed. An optical gain coefficient of 18 cm^{-1} was observed with the use of a C_{60} sensitizer under $E = 48$ V μm^{-1} at 633 nm.[99] Low-T_g PR polyacrylates containing

3-(6-nitrobenzoxazol-2-yl)indole as monolithic chromophores were also designed. For these polymers, a diffraction efficiency of 5.18% and optical gain of 27.4 cm^{-1} (net optical gain: 15.0 cm^{-1}) were observed with the use of 1 wt% of a TNF sensitizer under $E = 60\ V\ \mu m^{-1}$ at 632.8 nm (60.7 mW cm^{-2}).[100] Conjugated poly(phenylenevinylene)s incorporated with NLO chromophores as pendant groups were copolymerized with a small amount of macrocyclic zinc complexes (polymers 1, 2 and 4 in Figure 12). Optical gains of 47.7, 54.2 and 93.6 cm^{-1} (net optical gain: 35.5, 17.2 and 83.3 cm^{-1}) were obtained under a relatively low electric field of 45 V μm^{-1} at 632.8 nm for polymers 1, 2 and 4, respectively. Response times of 4.7, 0.45 and 0.094 s were obtained under $E = 60\ V\ \mu m^{-1}$ with illumination (2×1.6 mW cm^{-2}) at 632.8 nm for polymers 1, 2 and 4, respectively. Diffraction efficiencies between 10 and 23% were measured, and a higher diffraction efficiency of 23% was observed for polymer 4.[101] PR poly(p-phenylene-thiophene)s attached NLO groups (Figure 13) were designed. This PR polymer did not require the use of any photosensitizers, and an optical gain of 158 cm^{-1} at $E = 50\ V\ \mu m^{-1}$ and a diffraction efficiency of 68% at $E = 46\ V\ \mu m^{-1}$ were observed.[102] Multifunctional PR polyacrylates bearing five different monolithic chromophores (Figure 14) were designed. These monolithic chromophores consisted of carbazole and nitro groups, which were directly connected (PCzN) and bridged via azobenzene (PCzAN), stilbene (PCzSN), benzoxazole (PCzBN) and cyanostilbene (PCzCSN) groups. PCzN, PCzAN, PCzSN and PCzSCN gave positive optical gains, whereas PCzBN generated a negative gain. The authors attributed these phenomena to differences in the hole and electron mobilities.[103]

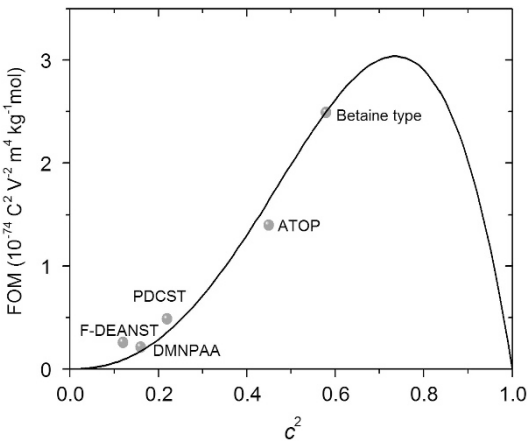

Figure 7 Plots of FOM of NLO dyes as a function of c^2. Solid curve was calculated using Equations (11)–(15) and (17). A full color version of this figure is available at *Polymer Journal* online.

Fully functionalized molecular glasses. A PR molecular glass consisting of a multifunctional conjugated carbazole trimer (Figure 2) was designed. An optical gain of 35.0 cm^{-1} (net gain of 26.8 cm^{-1}) was recorded under $E = 33\ V\ \mu m^{-1}$ at 532 nm.[53] The PR performance of a 2-dicyanomethylen-3-cyano-5,5-dimethyl-4-(4'-dihexylaminophenyl)-2,5-dihydrofuran (DCDHF-6 in Figure 15) molecular glass was also reported. The optical diffraction and gain of this molecular glass were measured with a C_{60} sensitizer at 905 nm.[104] PR molecular glasses consisting of dicarbazole-substituted triarylamine (DCTA) moieties connected to DCST chromophores via linker molecular chains with various lengths were designed (DCST-2C-DCTA, DCST-6C-DCTA and DCST-12C-DCTA in Figure 15). Their T_gs decreased and their PR optical gains increased by twofold starting from the 2-carbon atom linker to the 12-carbon atom linker.[105]

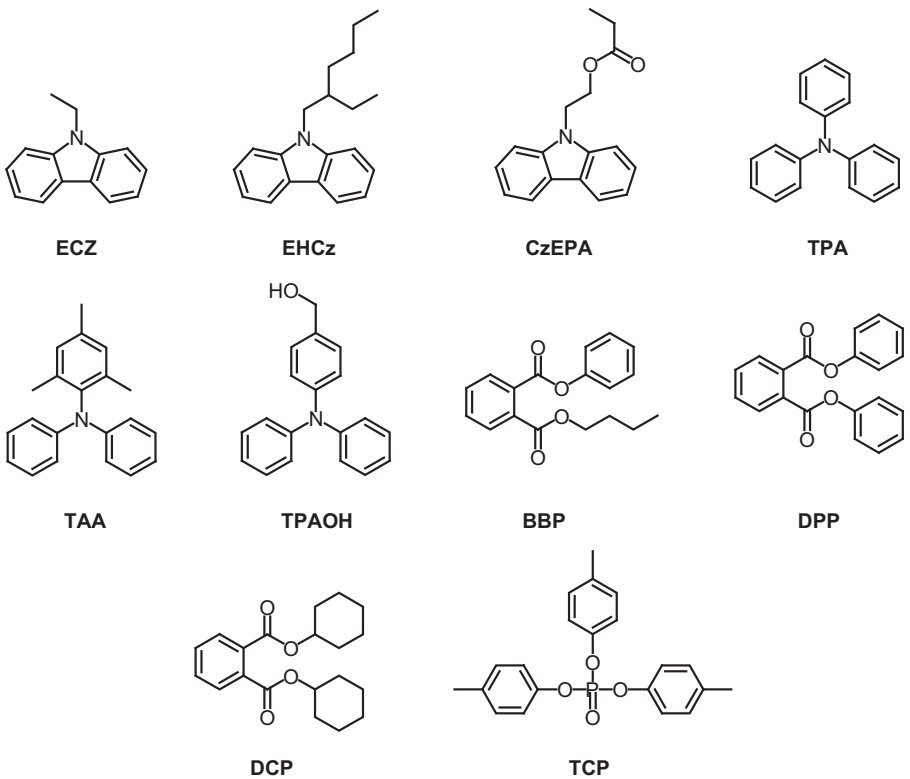

Figure 8 Structural formulae of plasticizers used to generate photorefractive composites.

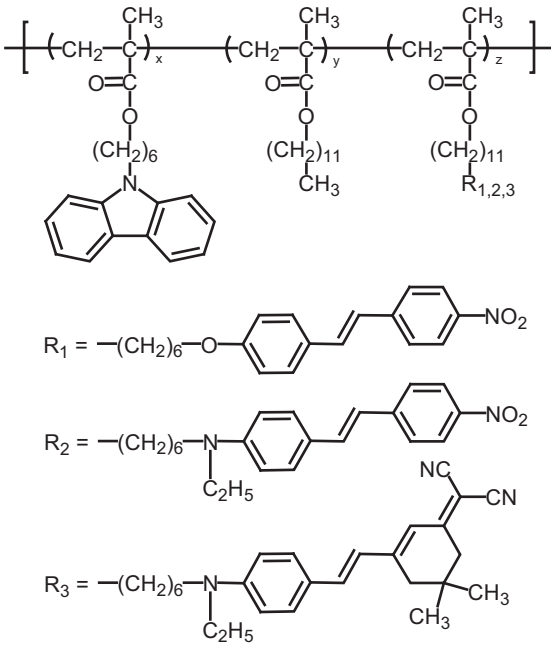

Figure 9 Fully functionalized polymer. Redrawn from an original illustration in Van Steenwinckel *el al.*[95]

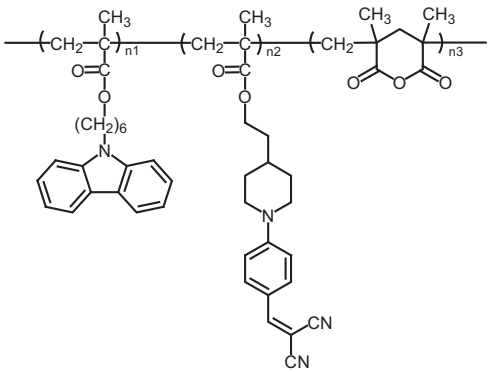

Figure 10 Fully functionalized polymer in Giang *et al.*[98]

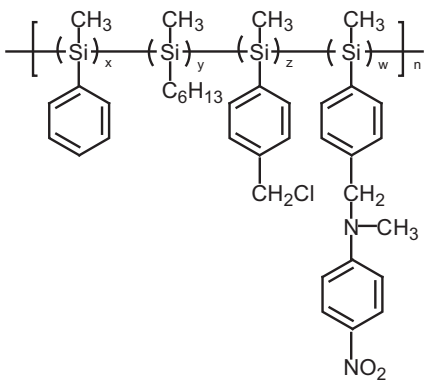

Figure 11 Fully functionalized polymer. Redrawn from an original illustration in Hendrickx *et al.*[99]

EFFECTS OF MODIFYING MOLECULAR STRUCTURES: MOLECULAR WEIGHT

A detailed investigation on the effects of altering polymer molecular weights (M_w and M_n) on PR performances was performed for PVK-based PR polymer composites of PVK/liquid crystal/fullerene with average M_ns ranging from 10 000 to 66 000 g mol^{-1}[106] and PVK/7-DCST/ECZ/TNF with average M_ws ranging from 23 000 to 412 000 g mol^{-1}[107] and from 23 000 to 1270 000 g mol^{-1}.[44] An increase in optical gain was observed with an increase in average M_n for PVK/liquid crystal/fullerene.[106] Diffraction efficiencies, response rates and sensitivities all increased with increases in M_w,[44,107] except for $M_w = 1270\,000$,[44] as shown in Figure 16. This was attributed to the dimer cation sites that formed along longer polymer chains in PVK with higher molecular weights that worked as effective traps for hole charge carriers.[44,107]

EFFECTS OF ALTERING GRATING PITCHES

The effect of grating pitches on the optical diffraction, optical gain and response time of polymers was investigated for PVK/7-DCST/ECZ/PCBM.[44] As shown in Figure 17, a distinct increase in optical gain and decreases in diffraction efficiency and response time were observed with a decrease in grating pitches. With a decrease in grating pitch, the phase shift Φ between the refractive index modulation and illumination pattern increased, and the number of density of traps (N_T) and the resultant trap-limited space-charge field (E_q) decreased.

PHOTOCONDUCTIVITY AND RESPONSE TIMES

The response rate (inverse of the response time) of grating formation is an important feature for the performance of PR polymers. For example, this feature is important for video-rate applications such as dynamic three-dimensional (3D) holographic displays. Grating formation rates are significantly related to the photoconductivity of composites. The formation of light-induced grating has theoretically been investigated for inorganic PR materials by Kukhtarev *et al.*[14] Yeh[40] proposed the fundamental limit of the growth time τ for grating formation in inorganic PR materials using the following equation:

$$\tau = \frac{2\varepsilon_0 \varepsilon_r E_{sc}\, \hbar\omega}{e\Lambda \quad \alpha\phi I} \tag{18}$$

where E_{SC} is the space-charge field, $\hbar$ is Planck's constant, ω is the angular frequency, Λ is the grating pitch, ϕ is the photogeneration efficiency of the charge carriers and I is the incident light intensity. Here, all the processes of charge carrier transport and trapping are assumed to occur instantaneously after photogeneration of the charge carriers.

Alternatively, growth time is defined as the time needed to fill the traps by the photogenerated holes:

$$\tau = \frac{\alpha\phi I}{\hbar\omega} T_i \tag{19}$$

with

$$E_q = \frac{e\Lambda}{2\pi\varepsilon_0\varepsilon_r} T_i \tag{20}$$

result in the following expression for growth time:[108]

$$\tau = \frac{2\pi\varepsilon_0\varepsilon_r E_q \hbar\varpi}{e\Lambda \quad \alpha\phi I} \tag{21}$$

Here, E_q is a trap-limited space-charge field and T_i is the initial trap

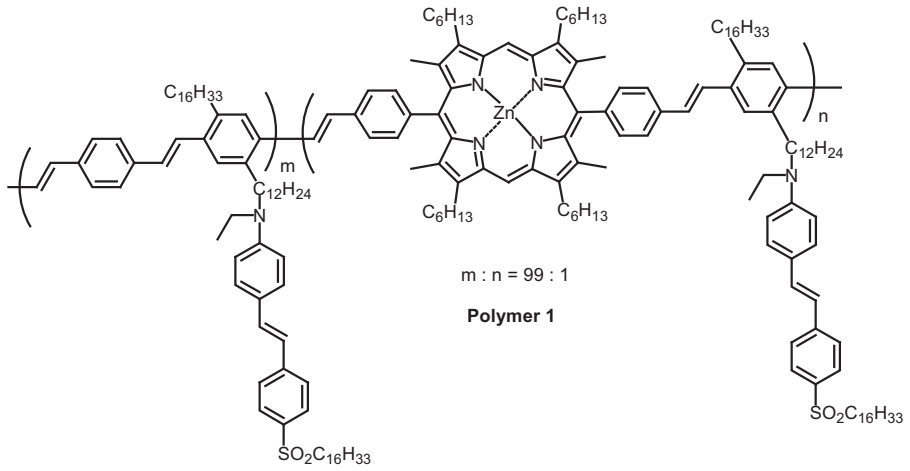

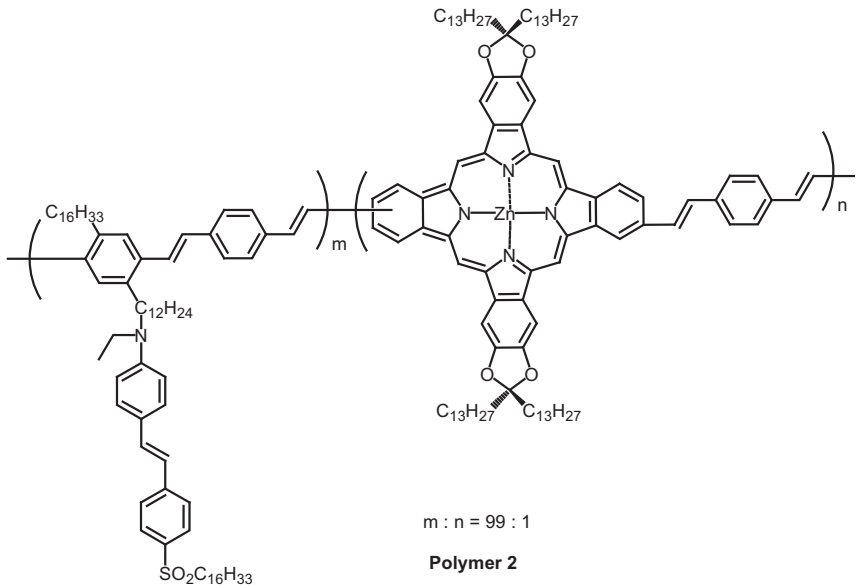

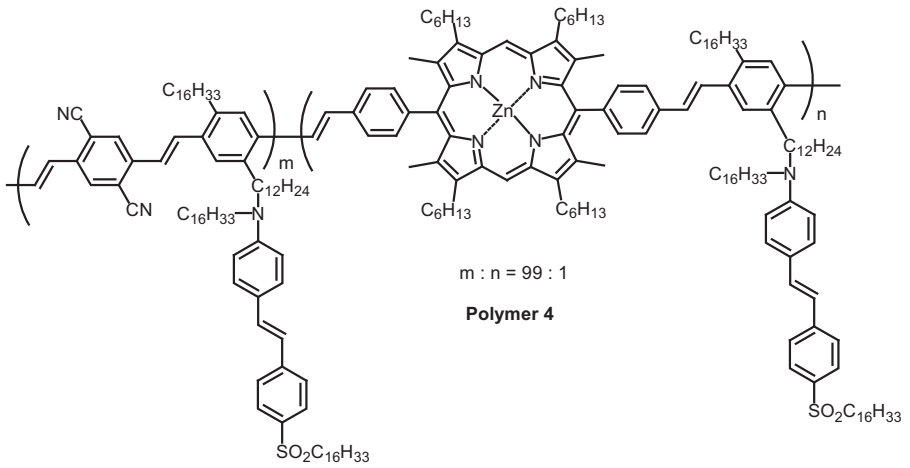

Figure 12 Fully functionalized polymer. Redrawn from an original illustration You *et al.*[101]

density in Schildkraut model.[109] Equation (20) is equivalent to Equation (9) when $T_i = N_T$.

For PVK-based PR composites of PVK/DMNPAA/TNF, the response times (the growth time in the literature) between 1 and 10 s depending on the applied electric field were measured. In contrast, Equations (18) and (21) predict the response times at a speed that is one to two orders of magnitude faster than the measured response times.[110]

Steady-state photocurrent is defined as $j_{ph} = \sigma_{ph} E$, and the internal photocurrent efficiency φ_{ph} is written using the following equation:[41,42,78,105]

$$\varphi_{ph}(E) = \frac{j_{ph} h\nu}{eI\alpha L} = \frac{\sigma_{ph} E h\nu}{eI\alpha L} \quad (22)$$

where σ_{ph} is the photoconductivity, E is the applied electric field, h is Planck's constant, ν is the light frequency, I is the intensity of light, α is the absorption coefficient and L is the thickness of the PR composite film.

The internal photocurrent efficiency φ_{ph} (E) is related to the photocarrier generation efficiency ϕ[108] through the following equation:

$$\varphi_{ph}(E) = G\phi = \frac{\varepsilon_r \varepsilon_0 E}{eLT_i}\phi \quad (23)$$

where G is the photoconductivity gain factor and T_i is the initial trap density in Schildkraut model.[109]

The response rate $\tau_G{}^{-1}$ can be evaluated from Equation (24) using Equations (19) and (20):

$$\frac{1}{\tau_G} = \frac{\sigma_{ph}}{\varepsilon_r \varepsilon_0} \quad (24)$$

The response rate $\tau_G{}^{-1}$ is related to photoconductivity σ_{ph} and the dielectric constant. Namely, Equation (24) shows that the PR response rate is linearly correlated to photoconductivity.

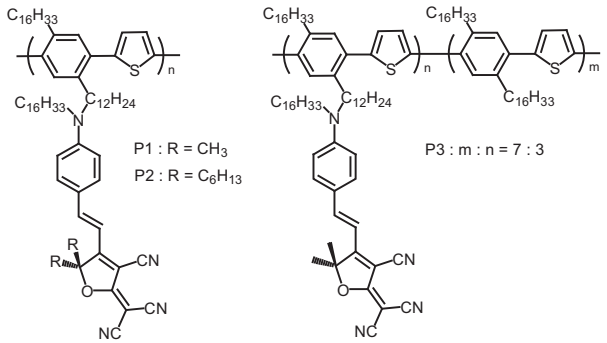

Figure 13 Fully functionalized polymer. Redrawn from an original illustration You *et al.*[102]

Response times of 4 or 5 ms were reported in PVK-based PR composites of PVK/7-DCST or AODCST/BBP/C_{60} at an extremely high electric field of 100 V μm^{-1} and under an illumination of 1 W cm^{-2}, respectively.[38] The same study also measured the photoconductivity of polymers generated with AODCST NLO chromophore cases; σ_{ph} = 700 pS cm^{-1} was measured at 100 V μm^{-1}. Assuming a dielectric constant ε_r of 3.5, Equation (24) predicts τ_G = 0.44 ms, which is one order of magnitude faster than the measured response time of 5 ms. A fast response time of 0.86 ms and an optical diffraction of 83% were reported at 60 V μm^{-1}, and under an illumination of 0.535 W cm^{-2} for PTAA-based PR composites of PTAA/PDCST/TAA/PCBM/Alq_3.[41] A σ_{ph} value of 8.9 nS cm^{-1} was simultaneously measured and predicted τ_G = 35 μs at 60 V μm^{-1} and under an illumination of 0.535 W cm^{-2}.[41]

In both of the estimates described above, response times (growth times) that were one or two orders of magnitude faster were predicted. This denotes that either the photoconductivity of the materials did not directly contribute to their PR response or that the large photocurrents limited the formation of effective space-charge fields.[41]

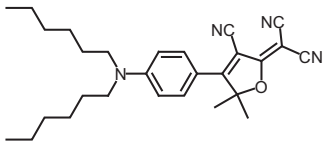

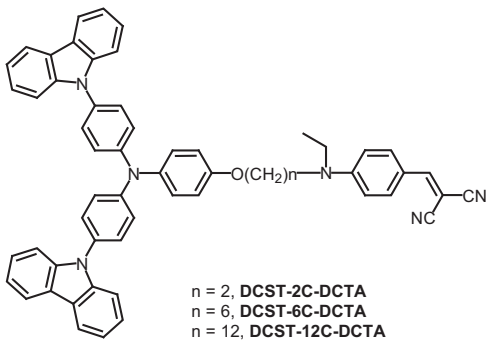

Figure 15 Fully functionalized polymer. Redrawn from an original illustration Gubler *et al.*[104] and He *et al.*[105]

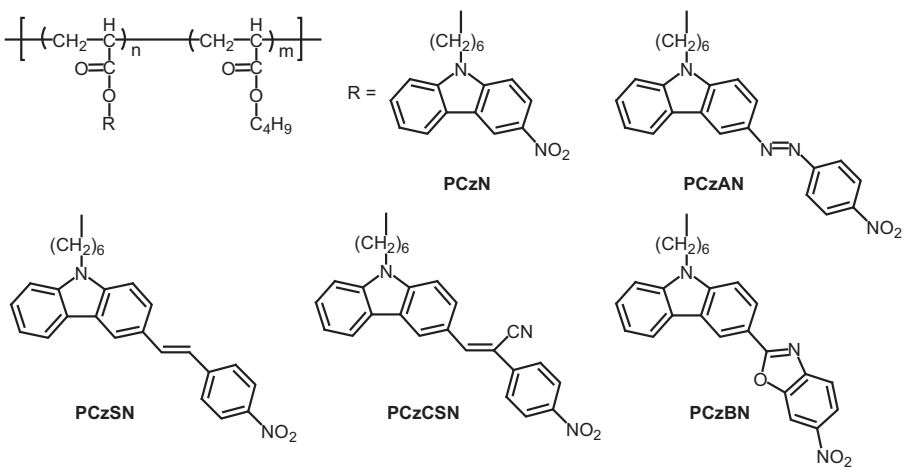

Figure 14 Fully functionalized polymers. Redrawn from an original illustration Hwang *et al.*[103]

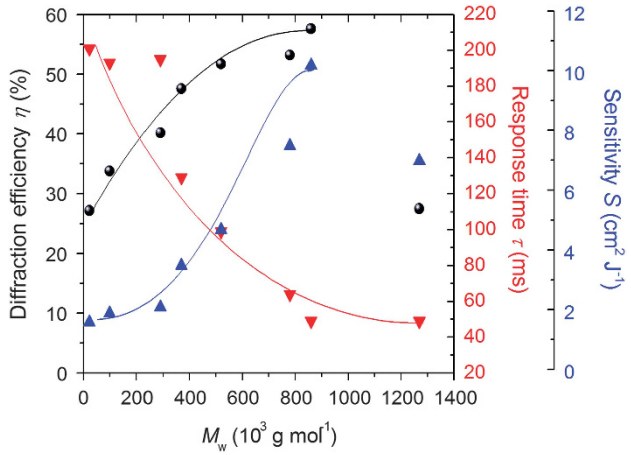

Figure 16 Dependence of diffraction efficiency η, response time τ and sensitivity S on the molecular weight of PVK. Original data were taken from Kinashi *et al.*[44] Solid circle, diffraction efficiency η; reverse triangle, response time τ; triangle, sensitivity S. Solid curve is a guide for the eyes.

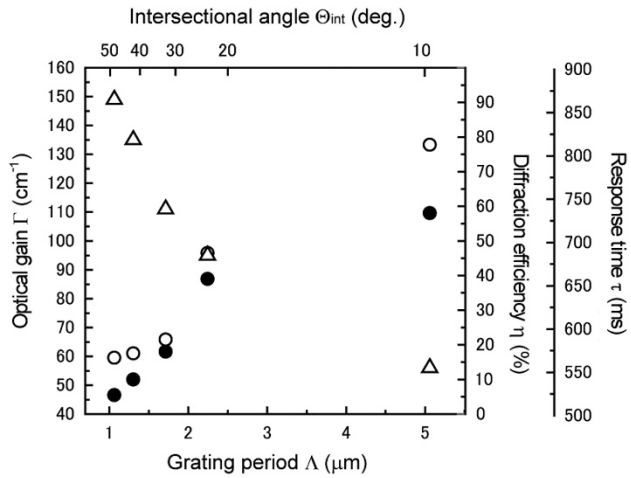

Figure 17 Plots of optical gains, diffraction efficiencies and response times as a function of grating pitch. Reproduced from Kinashi *et al.*[44] with permission from Wiley-VCH.

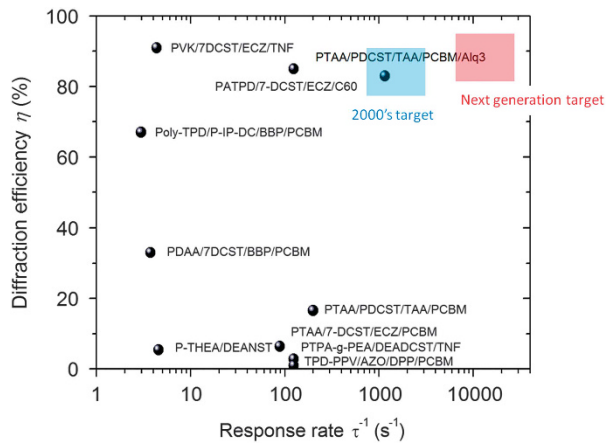

Figure 18 Plots between response rates and diffraction efficiencies. The data were taken from Table 1.

In a recent approach, which used a PTAA photoconductive polymer with a drift mobility in the order of 10^{-2}–10^{-3} cm^2 V^{-1} s^{-1}, Tsutsumi *et al.* successfully achieved a fast two-beam-coupling response with a response time of 350 μs and a decay time of 200 μs. These data were obtained by applying a rectangular electric field (maximum field: 60 V μm^{-1}) at 100 Hz cycling, which corresponded well to the rectangular response of a photocurrent with a response time of 367 μs and a decay time of 213 μs when the laser beam was cycled at a frequency of 100 Hz under a constant electric field of 60 V μm^{-1}.[41] As shown in Table 1, the authors also achieved a fast response time of 860 μs with 83% diffraction efficiency. These fast responses were ascribed to the control of the photocurrent flow using a second sensitizer (Alq_3).[41] A CT complex between PTAA and Alq_3 was believed to suppress the photocurrent flow, which improved the resulting response time. With a different mechanism, adding Alq_3 as a second electron trap improved the PR response of a material with a depression in the photocurrent.[79] The response rates and the diffraction efficiencies shown in Table 1 are plotted in Figure 18. Faster response times and high diffraction efficiencies could be simultaneously satisfied in some PR materials. We are now in a new stage where the response rates of materials exceed 1000 s^{-1} and have high diffraction efficiencies of over 80%. The next generation target is the development of materials with response rates that exceed 10 000 s^{-1} (response time faster than 100 μs).

PR RESPONSE IN A CENTROSYMMETRIC ENVIRONMENT

Asymmetric two-beam coupling is a unique feature of PR materials. A phase shift ($0 < \Phi \leqslant 90°$) between an illumination pattern and refractive modulation causes an asymmetric energy transfer in two-beam-coupling measurements. In PR media, the refractive index modulation is caused by Pockels effect based on the phase-shifted space-charge field. Thus, usual asymmetric energy transfer occurs in the presence of an external electric field. However, several reports on asymmetric two-beam-coupling gains without the application of an external electric field have been reported for carbazole-based PR polymers,[93,94,111,112] azobenzene derivatives in matrices[113] and carbazole–azobenzene monolithic compound-based PR polymers.[114–116] Asymmetric two-beam coupling has also been reported in high T_g non-poled PR polymers with carbazole and azobenzene moieties as pendant groups.[117] A large optical gain coefficient exceeding 1000 cm^{-1} was observed in a sol–gel matrix doped with Disperse Red 1 (DR1) in the absence of an external electric field.[113] Asymmetric energy transfer was found to occur in centrosymmetric media. A new model considering the influence of a Poynting vector on a photo-isomerization process was proposed to explain the asymmetric two-beam-coupling gain in the sol–gel matrix doped with DR1 in the absence of an external electric field.[113] On the basis of the coupled wave theory for thick hologram gratings proposed by Kogelnik,[36] Kawabe *et al.*[118,119] reported a possible mechanism for this asymmetric energy transfer without charge redistribution in the matrix. They proposed that beam intensity variations, such as asymmetric energy transfer in a PR medium, could be reproduced if a phase difference between the refractive index (phase) modulation φ_P and the absorption (amplitude) modulation φ_A was 90 degrees.[119]

OPTICAL APPLICATIONS

Updatable holographic displays

Updatable holographic displays are one of the most attractive applications of PR polymer composites. Holograms, which display full-parallax 3D images, were discovered by Gabor[120] in 1948. Figure 19 shows the typical schematic diagram of a hologram

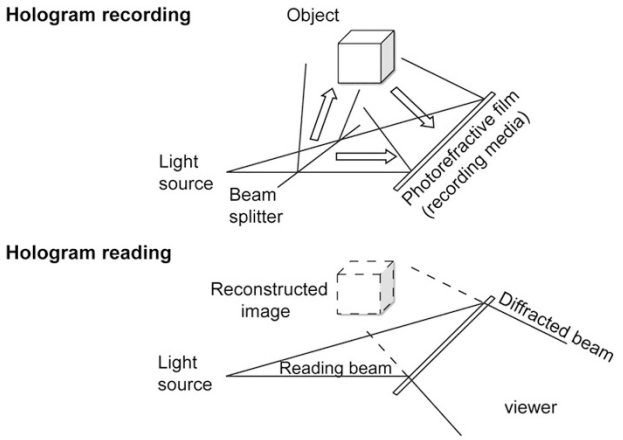

Figure 19 The principle of hologram recording and reading. By courtesy of Dr HN Giang.

recording and reconstruction. In the recording process, reflected light from the object and the reference light is interfered in the recording media (PR film), and the interference pattern is recorded on PR film. During the reading process, a hologram is reconstructed from the recording media (PR film) using reading light. People can see completely reproduced full-parallax 3D images using holography without wearing any special eyeglasses. Conventional holograms were recorded on silver halides, photopolymers and dichromated gelatin.[121] However, these holograms lacked the capability for image-updating. Recently, PR polymer films have opened a new door for the development of updatable 3D holographic displays based on dynamic holography. Large-scale holographic display devices can now be easily processed, and video-rate PR responses can be achieved. Thus, PR polymer-based PR devices are highly desired for the development of real-time 3D holographic display systems.

Peyghambarian's group at the University of Arizona, USA, demonstrated the development of updatable 3D holographic displays using a combination of a PR polymer device and a holographic stereogram technique.[122–125] They succeeded in developing a long-persistence updatable hologram system, which could be viewed for minutes to hours by controlling the T_g of the PR polymer device. They recorded 100 hogels for 2–4 min using a holographic stereographic technique to reconstruct a monochromatic hologram, which could be observed for 3 h on a 100 mm × 100 mm PR device consisting of PATPD-CAAN/FDCST/ECZ (50/30/20 by wt.).[122,123] By using a pulse laser with a duration time of 6 ns that delivered 200 mJ per pulse at a repetition rate of 50 Hz, 100 hogels were recorded for 2 s to reconstruct multicolor holograms on a 300 mm diameter PR device consisting of PATPD-CAAN/FDCST/ECZ/PCBM (49.5/30/20/0.5 by wt.).[124] The hologram had a brightness of 2500 cd m^{-2}, reduced laser power of 20 mW CW laser, and reported an improvement in resolution and a three-color hologram.[125]

Tsutsumi *et al.*[126–128] at the Kyoto Institute of Technology, Japan, also demonstrated the development of an updatable 3D hologram and holographic stereogram images using a monolithic compound containing carbazole–azobenzene without a bias-field. In the updatable 3D holographic stereogram display device, 50–100 elemental holograms (hogels) were recorded every 300 ms on a device made of a monolithic compound using a green laser; the recorded 3D holographic stereogram was reconstructed using a yellow–orange or red laser.[127] Recording and reconstruction of the hologram were operated using a software called Holographic Stereogram, KIT (Kyoto Institute of Technology, Kyoto, Japan).[127] The authors also reconstructed an updatable hologram of a coin and a 2D hologram of an object image from a special light modulator using a PVK-based PR polymer composite of PVK/7-DCST/CzEPA/TNF (44/35/20/1 by wt.).[91] Using the same PR polymer device, they reconstructed a dynamic 2D hologram with an object image that was supplied from a spatial light modulator at a refresh time of 1 s using the same PVK PR device,[129] and a 50 ms response time using a PDAS-based PR composite of PDAS/FDSCT/ECZ/PCBM (44/35/20/1 by wt.).[62,63] Video-rate updatable hologram imaging was successfully demonstrated on a PDAS-based PR composite because of the higher hole mobility of PDAS, which was in the order of 10^{-4}–10^{-3} cm^2 V^{-1} s^{-1}.[62] 2D holographic images were reconstructed using a 100 mm × 100 mm device that consisted of a PDAA-based PR composite of PDAA/7-DCST/BBP/PCBM (55/40/4/1 by wt.).[43]

Holographic optical coherence imaging

Holographic optical coherence imaging (HOCI) is based on the capture of depth-resolved images from a turbid and highly scattered medium using coherence gating.[130] This technique is a non-invasive imaging tool that can be used to map the depth profile of biological tissues. Biological tissues usually demonstrate absorbance in the visible region, but the absorption is reduced in the therapeutic window, which spans from 600 to 1300 nm.[131] The transparency window of biological tissues, which is used for biological mapping, is in the near-infrared region at ~700–900 nm. A short-coherence light source, such as a femtosecond NIR laser, is commonly used. By using coherence-gated holographic imaging, image-bearing light captured on a PR polymer medium can be read out as a hologram image in real time without necessitating any further computational steps. Thus, the HOCI technique based on PR polymer devices is a method that can be used for image capturing in a purely optical manner and in real time, in contrast to optical coherence tomography, confocal scanning microscopy and HOCI by digital holography.

Volumetric visualization of a 740-μm rat osteogenic sarcoma tumor spheroid was successfully demonstrated using HOCI with an infrared femtosecond laser at 830 nm.[130]

PR phase conjugators

PR media have features of phase conjugators, which can produce phase-conjugate waves of incident electromagnetic waves.[12] A phase-conjugate wave propagates back to a reversed direction in space and is referred as a time-reversed wave. A phase conjugator can restore a distorted wave. By using a degenerate four-wave mixing technique, a distorted image passing through a phase-disordered medium was interfered with a reference beam in a PSX-Cz/DB-IP-DC/TNF PR composite[132] and a carbazole–azobenzene monolithic compound-based PR medium.[116] A counter-propagated probe beam could read out the phase-conjugate wave of the distorted image as a diffracted wave. A diffracted phase-conjugated distorted image was propagated back through a phase disorder medium to restore the original wave front.[116,132]

Optical computing and image amplification

PR materials can be used in optical information processing, such as processing of real-time optical data, detecting image correlations, optical interconnections, optical neural networks and optical computing.[12]

PR optical gains due to asymmetric energy transfer are a unique feature that can be utilized to amplify original images. PR composites consisting of ferroelectric liquid crystals and photoconductive chiral

compounds were shown to possess large optical gains exceeding 1200 cm^{-1} with a response time of 1 ms.[133] Real-time dynamic amplification of an optical image over 30 f.p.s. was also demonstrated.[133]

CONCLUSIONS AND FUTURE PERSPECTIVES

In this report, the molecular design of organic PR polymers was reviewed. Tremendous work on the investigation of organic photorefractivity has been performed over the past two decades. Many studies have been dedicated to improve PR response times. Response times were in the order of seconds in the first stage but are now in the order of hundreds of microseconds for asymmetric energy transfer and optical diffraction of PTAA PR composites. PTAA was first developed in the field of organic field-effect transistors. Thus, the development of materials in different fields will merge together to trigger the development of newer materials.

Organic sensitizers are important components of organic PR polymers. Several types of fullerene-based sensitizers have been developed, and graphene, PBI and DiPBI have been recently introduced as new sensitizers. Among these compounds, a fullerene derivative of PCBM has been one of the most successful sensitizers. Many types of organic NLO chromophores have been synthesized for use in the generation of organic PR materials. In addition to the electro-optic effect, NLO chromophores are required to possess large optical anisotropy properties because of the molecular orientation of NLO chromophores due to the presence of space-charge fields (orientational enhancement). FOMs including an electro-optic effect and optical anisotropy were introduced to evaluate the application of NLO chromophores in PR polymers. However, crystallization of NLO chromophores in composites degraded the performance of the PR materials. To avoid crystallization of the NLO chromophores, many types of NLO chromophores have been designed and investigated. We have yet to find the most favorable NLO chromophore for use in PR materials.

Holographic display devices are one of the practical applications of organic PR polymers. However, the robustness of PR devices in high electric fields is a key issue for their use in practical applications. In some types of centrosymmetric materials, asymmetric energy transfer with extremely large optical gains and high diffraction efficiencies have been reported. The development of updatable holograms and holographic stereograms was clearly demonstrated using a monolithic compound containing carbazole and azobenzene under unbiased conditions. The use of holographic display devices without bias fields is very attractive for practical applications.

In parallel to studies on the design of PR materials, fundamental studies on the hole and electron transport in each manifold of PR amorphous materials should also be examined because there is a need for a deeper understanding of these phenomena. For example, the density of state for hole transport, which significantly affects hole transport and mobility, has not been directly measured. Future studies on density-of-state measurements are extensively encouraged.

CONFLICT OF INTEREST

The author declares no conflict of interest.

ACKNOWLEDGEMENTS

NT acknowledges the program for the Strategic Promotion of Innovative Research and Development (S-Innovation) at the Japan Science and Technology Agency (JST) for their financial support.

1 Ducharme, S., Scott, J. C., Twieg, R. J. & Moerner, W. E. Observation of the photorefractive effect in a polymer. *Phys. Rev. Lett.* **66**, 1846–1849 (1991).
2 Tang, C. W. & Vanslyke, S. A. Organic electroluminescent diodes. *Appl. Phys. Lett.* **51**, 913–915 (1987).
3 Burroughes, J. H., Bradley, D. D. C., Brown, A. R., Marks, R. N., Mackay, K., Friend, R. H., Burns, P. L. & Holmes, A.B. Light-emitting diodes based on conjugated polymers. *Nature* **347**, 539–541 (1990).
4 Friend, R. H., Gymer, R. W., Holmes, A. B., Burroughes, J. H., Marks, R. N., Taliani, C., Bradley, D. D. C., Dos Santos, D. A., Brédas, J. L., Lögdlund, M. & Salaneck, W. R. Electroluminescence in conjugated polymers (Review). *Nature* **397**, 121–128 (1999).
5 Kraft, A., Grimsdale, A. C. & Holmes, A. B. Electroluminescent conjugated polymers—seeing polymers in a new light (review). *Angew. Chem. Int. Ed. Engl.* **37**, 402–428 (1998).
6 Grimsdale, A. C., Chan, K. L., Martin, R. E., Jokisz, P. G. & Holmes, A. B. Synthesis of light-emitting conjugated polymers for applications in electroluminescent devices (Review). *Chem. Rev.* **109**, 897–1091 (2009).
7 Sirringhaus, H., Tessler, N. & Friend, R. H. Integrated optoelectronic devices based on conjugated polymers. *Science* **280**, 1741–1744 (1998).
8 Tang, C. W. Two-layer organic photovoltaic cell. *Appl. Phys. Lett.* **48**, 183–185 (1986).
9 Yu, G., Gao, J., Hummelen, J. C., Wudl, F. & Heeger, A. J. Polymer photovoltaic cells: enhanced efficiencies via a network of internal donor-acceptor heterojunctions. *Science* **270**, 1789–1791 (1995).
10 Brabec, C. J., Sariciftci, N. S. & Hummelen, J. C. Plastic solar cells. *Adv. Funct. Mater.* **11**, 15–26 (2001).
11 Kojima, A., Teshima, K., Shirai, Y. & Miyasaka, T. Organometal halide perovskites as visible-light sensitizers for photovoltaic cells. *J. Am. Chem. Soc.* **131**, 6050–6051 (2009).
12 Yeh, P. *Introduction to Photorefractive Nonlinear Optics* (Wiley Interscience, New York, NY, USA, 1993).
13 Ashkin, A., Boyd, G. D., Dziedzic, J. M., Smith, R. G., Ballman, A. A., Levinstein, J. J. & Nassau, K. Optically-induced refractive index inhomogeneities in $LiNbO_3$ and $LiTaO_3$. *Appl. Phys. Lett.* **9**, 72–74 (1966).
14 Kukhtarev, N. V., Markov, V. B., Odulov, S. G., Soskin, M. S. & Vinetskii, V. L. Holographic storage in electrooptic crystals. I. Steady state. *Ferroelectrics* **22**, 949–960 (1979).
15 Meerholtz, K., Volodin, B. L., Sandalphon, Kippelen, B. & Peyghambarian, N. A photorefractive polymer with high optical gain and diffraction efficiency near 100%. *Nature* **371**, 497–500 (1994).
16 Moerner, W. E. & Silence, S. M. Polymeric photorefractive materials. *Chem. Rev.* **94**, 127–155 (1994).
17 Zhang, Y., Burzynski, R., Ghosal, S. & Casstevens, M. K. Photorefractive polymers and composites. *Adv. Mater.* **8**, 111–125 (1996).
18 Moerner, W. E., Grunnet-Jepsen, A. & Thompson, C. L. Photorefractive polymers. *Annu. Rev. Mater. Sci.* **27**, 585–623 (1997).
19 Zhang, Y., Wada, T. & Sasabe, H. Carbazole photorefractive materials. *J. Mater. Chem.* **8**, 809–828 (1998).
20 Zilker, S. J. Materials design and physics of organic photorefractive systems. *ChemPhysChem* **1**, 72–87 (2000).
21 Wang, Q., Wang, L. & Yu, L. Development of fully functionalized photorefractive polymers. *Macromol. Rapid Commun.* **21**, 723–745 (2000).
22 Kippelen, B. & Peyghambarian, N. Photorefractive polymers and their applications. *Adv. Polym. Sci.* **161**, 87–156 (2003).
23 Ostroverkhova, O. & Moerner, W. E. Organic photorefractives: mechanisms, materials, and applications. *Chem. Rev.* **104**, 3267–3314 (2004).
24 Sasaki, T. Photorefractive effect of liquid crystalline materials. *Polym. J.* **37**, 797–812 (2005).
25 Thomas, J., Norwood, R. A. & Peyghambarian, N. Non-linear optical polymers for photorefractive applications. *J. Mater. Chem.* **19**, 7476–7489 (2009).
26 Köber, S., Salvador, M. & Meerholz, K. Organic photorefractive materials and applications. *Adv. Mater.* **23**, 4725–4763 (2011).
27 Lynn, B., Blanche, P.-A. & Peyghambarian, N. Photorefractive polymers for holography. *J. Polym. Sci. B Polym. Phys.* **52**, 193–231 (2014).
28 Kippelen, B., Meerholz, K. & Peyghambarian, N. in *Nonlinear Optics of Organic Molecules and Polymers* (eds Nalwa, H. S. & Miyata, S.) (CRC Press, Boca Raton, IL, USA, 1997).
29 Meerholz, K., Kippelen, B. & Peyghambarian, N. in *Photonic Polymer Systems* (eds Wise, D. L., Wnek, G. E., Trantolo, D. J., Cooper, T. M. & Gresser, J. D.) (Marcel Dekker, New York, NY, USA, 1998).
30 Bittner, R. & Meerholz, K. in *Springer Series in Optical Sciences* Vol. 114 (eds Günter, P. & Huignard, J.-P.) 419–486 (Springer, Berlin, Germany, 2006).
31 Kippelen, B. in *Springer Series in Optical Sciences* Vol. 114 (eds Günter, P. & Huignard, J.-P) 487–534 (Springer, Berlin, Germany, 2006).
32 Montemezzani, G., Medrano, C., Zgonik, M. & Günter, P. in *Springer Series in Optical Sciences* Vol. 72 (ed. Günter, P.) 301–373 (Springer, Berlin, Germany, 2000).
33 Simoni, F. & Lucchetti, L. in *Springer Series in Optical Sciences* Vol. 114 (eds Günter, P. & Huignard, J.-P.) 571–603 (Springer, Berlin, Germany, 2006).
34 Tsutsumi, N. in *Photorefractive Polymer in Encyclopedia of Polymeric Nanomaterials* (eds Kobayashi, S. & Müllen, K.) (Springer-Verlag, Berlin, Heidelberg, Germany, 2014).

35 Blanche, P.-A. in *Optical Properties of Functional Polymers and Nano Engineering Applications* (eds Jain, V. & Kokil, A.) Ch. 3, 27–60 (CRC Press, Boca Raton, USA, 2015).
36 Kogelnik, H. Coupled wave theory for thick hologram gratings. *Bell Syst. Tech. J.* **48**, 2909–2947 (1969).
37 Günter, P. & Huignard, J.-P. in *Photorefractive Materials and Their Applications* Vols. I and II, 1988 (Springer-Verlag, Berlin, Germany, 1989).
38 Wright, D., Díaz-García, M. A., Casperson, J. D., DeClue, M. & Moerner, W. E. High-speed photorefractive polymer composites. *Appl. Phys. Lett.* **73**, 1490–1492 (1998).
39 Kinashi, K., Shinkai, H., Sakai, W. & Tsutsumi, N. Photorefractive device using self-assembled monolayer coated indium-tin-oxide electrodes. *Org. Electron.* **14**, 2987–2993 (2013).
40 Yeh, P. Fundamental limit of the speed of photorefractive effect and its impact on device applications and material research. *Appl. Opt.* **24**, 602–604 (1987).
41 Tsutsumi, N., Kinashi, K., Masumura, K. & Kono, K. Photorefractive dynamics in poly (triarylamine)-based polymer composites. *Opt. Express* **23**, 25158–25170 (2015).
42 Tsutsumi, N., Kinashi, K., Masumura, K. & Kono, K. Photorefractive performance of poly(triarylamine)-based polymer composites: an approach from the photoconductive properties. *J. Polym. Sci. B Polym. Phys.* **53**, 502–508 (2015).
43 Giang, H. N., Kinashi, K., Sakai, W. & Tsutsumi, N. Photorefractive response using composite based on poly(4-(diphenylamino)benzyl acrylate) and real-time holographic application. *Polym. J.* **46**, 59–66 (2014).
44 Kinashi, K., Wang, Y., Sakai, W. & Tsutsumi, N. Optimization of photorefractivity based on poly(N-vinylcarbazole) composites: an approach from the perspectives of chemistry and physics. *Macromol. Chem. Phys.* **214**, 1789–1797 (2013).
45 Cao, Z., Abe, Y., Nagahama, T., Tsuchiya, K. & Ogino, K. Synthesis and characterization of polytriphenylamine based graft polymers for photorefractive application. *Polymer* **54**, 269–276 (2013).
46 Thomas, J., Fuentes-Hernandez, C., Yamamoto, M., Cammack, K., Matsumoto, K., Walker, G. A., Barlow, S., Kippelen, B., Meredith, G., Marder, S. R. & Peyghambarian, N. Bis triarylamine polymer-based composites for photorefractive applications. *Adv. Mater.* **16**, 2032–2036 (2004).
47 Moon, I. K., Choi, J. & Kim, N. High-performance potorefractive composite based on non-conjugated main-chain, hole-transporting polymer. *Macromol. Chem. Phys.* **214**, 478–485 (2013).
48 Okamoto, K., Nomura, T., Park, S. H., Ogino, K. & Sato, H. Synthesis and characterization of photorefractive polymer containing electron transport material. *Chem. Mater.* **11**, 3279–3284 (1999).
49 Mecher, E., Gallego-Gómez, F., Tillmann, H., Hörhold, H.-H., Hummelen, J. C. & Meerholz, K. Near-infrared sensitivity enhancement of photorefractive polymer composites by pre-illumination. *Nature* **418**, 959–964 (2002).
50 Zhang, Y., Cui, Y. & Prasad, P. N. Observation of photorefractivity in a fullerene-doped polymer composite. *Phys. Rev. B* **46**, 9900–9902 (1992).
51 Tsutsumi, N., Dohi, A., Nonomura, A. & Sakai, W. Enhanced performance of photorefractive poly(N-vinyl carbazole) composites. *J. Polym. Sci. B Polym. Phys.* **49**, 414–420 (2011).
52 Tsutsumi, N. & Miyazaki, W. Photorefractive performance of polycarbazoylethylacrylate composites with photoconductive plasticizer. *J. Appl. Phys.* **106**, 083113 (2009).
53 Zhang, Y., Wang, L., Wada, T. & Sasabe, H. Monolithic carbazole oligomer exhibiting efficient photorefractivity. *Appl. Phys. Lett.* **70**, 2949–2951 (1997).
54 Nishio, A., Wasai, K. & Tsutsumi, N. Synthesis and photorefractive properties of novel photoconductive low-molecular-weight glass compounds. *Kobunshi Ronbunshu* **60**, 725–732 (2003).
55 Tsutsumi, N., Eguchi, J. & Sakai, W. High performance photorefractive molecular glass composites in reflection gratings. *Chem. Phys. Lett.* **408**, 267–273 (2005).
56 Choi, J., Ji, S.-H., Choi, C.-S., Oh, J.-W., Kim, F.S. & Kim, N. Enhanced photorefractive performance of polymeric composites through surface plasmon effects of gold nanoparticles. *Opt. Lett.* **39**, 4571–4574 (2014).
57 Moon, J.-S., Liang, Y., Stevens, T. E., Monson, T. C., Huber, D. L., Mahala, B. D. & Winiarz, J. G. Off-resonance photosensitization of a photorefractive polymer composite using PbS nanocrystals. *J. Phys. Chem. C* **119**, 13827–13835 (2015).
58 Ego, C., Grimsdale, A. C., Uckert, F., Yu, G., Sranov, G. & Müllen, K. Triphenylamine-substituted polyfluorene—a stable blue-emitting with improved charge injection for light-emitting diodes. *Adv. Mater.* **14**, 809–811 (2002).
59 Ogino, K., Nomura, T., Shichi, T., Park, S.-H., Sato, H., Aoyama, T. & Wada, T. Synthesis of polymers having tetraphenyldiaminobiphenyl units for a host polymer of photorefractive composite. *Chem. Mater.* **9**, 2768–2775 (1997).
60 Köber, S., Gallego-Gomez, F., Salvador, M., Kooistra, F. B., Hummelen, J. C., Aleman, K., Mansurovac, S. & Meerholz, K. Influence of the sensitizer reduction potential on the sensitivity of photorefractive polymer composites. *J. Mater. Chem.* **20**, 6170–6175 (2010).
61 Tsutsumi, N., Murao, T. & Sakai, W. Photorefractive response of polymeric composites with pendant triphenyl amine moiety. *Macromolecules* **38**, 7521–7523 (2005).
62 Tsujimura, S., Kinashi, K., Sakai, W. & Tsutsumi, N. High-speed photorefractive response capability in triphenylamine polymer-based composites. *Appl. Phys. Express* **5**, 064101 (2012).
63 Tsujimura, S., Kinashi, K., Sakai, W. & Tsutsumi, N. Recent advances in photorefractivity of poly(4-diphenylamino)styrene composites: wavelength dependence and dynamic holographic images. *Jpn. J. Appl. Phys.* **53**, 082601 (2014).
64 Giang, H. N., Kinashi, K., Sakai, W. & Tsutsumi, N. Triphenylamine photoconductive polymers for high performance photorefractive devices. *J. Photochem. Photobiol. A* **291**, 26–33 (2014).
65 Meltz, P. J. Photogeneration in trinitrofluorenone-poly(N-vinylcarbazole). *J. Chem. Phys.* **57**, 1684–1699 (1972).
66 Mort, J. & Pai, D. M. *Photoconductivity and Related Phenomena* (Elsevier, New York, NY, USA, 1976).
67 Silence, S. M., Walsh, C. A., Scott, J. C. & Moerner, W. E. C_{60} sensitization of a photorefractive polymer. *Appl. Phys. Lett.* **61**, 2967–2969 (1992).
68 Zhang, Y., Spencer, C. A., Ghosal, S., Casstevens, M. K. & Burzynski, R. Thiapyrylium dye sensitization of photorefractivity in a polymer composite. *Appl. Phys. Lett.* **64**, 1908–1910 (1994).
69 Zhang, Y., Spencer, C. A., Ghosal, S., Casstevens, M. K. & Burzynski, R. Photorefractive properties of a thiapyrylium-dye-sensitized polymer composite. *J. Appl. Phys.* **76**, 671–679 (1994).
70 Dulmage, W. J., Light, W. A., Marino, S. J., Salzberg, C. D., Smith, D. L. & Staudenmayer, W. J. An aggregate organic photoconductor. I. Chemical composition, preparation, physical structure, and optical properties. *J. Appl. Phys.* **49**, 5543–5554 (1978).
71 Borsenberger, P. M., Chowdry, A., Hoesterey, D. C. & Mey, W. An aggregate organic photoconductor. II. Photoconduction properties. *J. Appl. Phys.* **49**, 5555–5564 (1978).
72 Vannikov, A. V., Grishina, A. D., Shapiro, B. I., Pereshivko, L. Ya., Krivenko, T. V., Savel'ev, V. V., Berendyaev, V. I. & Rychwalski, R. W. Photorefractive composites based on nanocrystalline carbocyanine dye J-aggregates with a fast response time. *High Energy Chem.* **37**, 410–416 (2003)
73 Ortiz, J., Fernández-Lázaro, F., Sastre-Santos, Á., Quintana, J. A., Villalvilla, J. M., Boj, P., Díaz-García, M. A., Rivera, J. A., Stepleton, S. E., Cox, C. T. Jr & Echegoyen, L. Synthesis and electrochemical and photorefractive properties of new trinitrofluorenone-C_{60} photosensitizers. *Chem. Mater.* **16**, 5021–5026 (2004).
74 Martín-Gomis, L., Ortiz, J., Fernández-Lázaro, F., Sastre-Santos, Á., Elliott, B. & Echegoyen, L. Synthesis and characterization of new trinitrofluorene–fullerene dyads as photosensitizers in photorefractive polymer materials. Redox behavior and charge-transfer properties. *Tetrahedron* **62**, 2102–2109 (2006).
75 Tsutsumi, N., Ito, Y. & Sakai, W. Effect of sensitizer on photorefractive nonlinear optics in poly(N-vinylcarbazole) based polymer composites. *Chem. Phys.* **344**, 189–194 (2008).
76 Gallego-Gomez, F., Quintana, J. A., Villalvilla, J. M., Díaz-García, M. A., Martín-Gomis, L., Fernandez-Lazaro, F. & Sastre-Santos, Á. Phthalocyanines as efficient sensitizers in low-Tg hole-conducting photorefractive polymer composites. *Chem. Mater.* **21**, 2714–2720 (2009).
77 Grishina, A. D., Krivenko, T. V., Savel'ev, V. V., Rychwalski, R. W. & Vannikov, A. V. Photoelectric, nonlinear optical, and photorefractive properties of polyvinylcarbazole composites with graphene. *High Energy Chem.* **47**, 46–52 (2013).
78 Chantharasupawong, P., Christenson, C. W., Philip, R., Zhai, L., Winiarz, J., Yamamoto, M., Tetard, L., Naire, R. R. & Thomas, J. Photorefractive performances of a graphene-doped PATPD/7-DCST/ECZ composite. *J. Mater. Chem. C* **2**, 7639–7647 (2014).
79 Christenson, C. W., Thomas, J., Blanche, P.-A., Voorakarana, R., Norwood, R. A., Yamamoto, M. & Peyghambarian, N. Grating dynamics in a photorefractive polymer with Alq_3 electron traps. *Opt. Express* **18**, 9358–9365 (2010).
80 Ditte, K., Jiang, W., Schemme, T., Denz, C. & Wang, Z. Innovative sensitizer DiPBI outperforms PCBM. *Adv. Mater.* **24**, 2104–2108 (2012).
81 Nguyen, T. V., Giang, H. N., Kinashi, K., Sakai, W. & Tsutsumi, N. Macromol. Chem. Phys. *Macro. Chem. Phys.* **217**, 85–91 (2016).
82 Yesodha, S. K., Pillai, C. K. S. & Tsutsumi, N. Stable polymeric materials for nonlinear optics: a review based on azobenzene systems. *Prog. Polym. Sci.* **29**, 45–74 (2004).
83 Moerner, W. E., Silence, S. M., Hache, F. & Bjorklund, G. C. Orientationally enhanced photorefractive effect in polymers. *J. Opt. Soc. Am. B* **11**, 320–330 (1994).
84 Wortmann, R., Poga, C., Twieg, R. J., Geletneky, C., Moylan, C. R., Lundquist, P. M., DeVoe, R. G., Cotts, P. M., Horn, H., Rice, J. E. & Burland, D. M. Design of optimized photorefractive polymers: a novel class of chromophores. *J. Chem. Phys.* **105**, 10637–10647 (1996).
85 Meyers, F., Marder, S. R., Pierce, B. M. & Brédas, J. L. Electric field modulated nonlinear optical properties of donor-acceptor polyenes: sum-over-states investigation of the relationship between molecular polarizabilities (α, β, and γ) and bond length alternation. *J. Am. Chem. Soc.* **116**, 10703–10714 (1994).
86 Beckmann, S., Etzbach, K.-H., Krämer, P., Lukaszuk, K., Matschiner, R., Schmidt, A. J., Schuhmacher, P., Sens, R., Seybold, G., Wortmann, R. & Würthner, F. Electrooptical chromophores for nonlinear optical and photorefractive applications. *Adv. Mater.* **11**, 536–541 (1999).
87 Würthner, F., Wortmann, R. & Meerholz, K. Chromophore design for photorefractive organic materials. *Chemphyschem* **3**, 17–31 (2002).
88 Kippelen, B., Meyers, F., Peyghambarian, N. & Marder, S. R. Chromophore design for photorefractive applications. *J. Am. Chem. Soc.* **119**, 4559–4560 (1997).
89 Marder, S. R., Kippelen, B., Jen, A. K.-Y. & Peyghambarian, N. Design and synthesis of chromophores and polymers for electro-optic and photorefractive applications. *Nature* **388**, 845–851 (1997).
90 Gieseking, R. L., Risko, C. & Bréda, J.-L. Distinguishing the effects of bond-length alternation versus bond-order alternation on the nonlinear optical properties of π-conjugated chromophores. *Phys. Chem. Lett.* **6**, 2158–2162 (2015).
91 Tsutsumi, N., Kinashi, K., Nonomura, A. & Sakai, W. Quickly updatable hologram images using poly(*N*-vinyl carbazole) (PVCz) photorefractive polymer composite. *Materials* **5**, 1477–1486 (2012).
92 Tsujimura, S., Fujihara, T., Sassa, T., Kinashi, K., Sakai, W., Ishibashi, K. & Tsutsumi, N. Enhanced photoconductivity and trapping rate through control of bulk state in organic triphenylamine-based photorefractive materials. *Org. Electron.* **15**, 3471–3475 (2014).

93 Tsutsumi, N. & Shimizu, Y. Asymmetric two beam coupling with high optical gain and high beam diffraction in external field free polymer composites. *Jpn. J. Appl. Phys.* **43**, 3466–3472 (2004).
94 Tsutsumi, N., Eguchi, J. & Sakai, W. Asymmetric energy transfer and diffraction efficiency of novel molecular glass with carbazole moiety. *Opt. Mater.* **29**, 435–438 (2006).
95 Van Steenwinckel, D., Engels, C., Gubbelmans, E., Hendrickx, E., Samyn, C. & Persoons, A. Fully functionalized photorefractive polymethacrylates with net gain at 780 nm. *Macromolecules* **33**, 4074–4079 (2000).
96 Engels, C., Van Steenwinckel, D., Hendrickx, E., Schaerlaekens, M., Persoons, A. & Samyn, C. Efficient fully functionalized photorefractive polymethacrylates with infrared sensitivity and different spacer lengths. *J. Mater. Chem.* **12**, 951–957 (2002).
97 Chen, Y., Zhang, B. & Wang, F. Photorefractive material based on a polymer containing photoconductors and nonlinear chromophores. *Opt. Commun.* **228**, 341–348 (2003).
98 Giang, H. N., Kinashi, K., Sakai, W. & Tsutsumi, N. Photorefractive composite based on a monolithic polymer. *Macromol. Chem. Phys.* **213**, 982–988 (2012).
99 Hendrickx, E., Van Steenwinckel, D., Persoons, A. & Watanabe, A. Photorefractive polysilanes functionalized with a nonlinear optical chromophore. *Macromolecules* **32**, 2232–2238 (1999).
100 Hwang, J., Sohn, J., Lee, J.-K., Lee, J.-H., Chang, J.-S., Lee, G. J. & Park, S. Y. Low T_g photorefractive polyacrylate containing 3-(6-nitrobenzoxazol-2-yl)indole as a monolithic chromophore. *Macromolecules* **34**, 4656–4658 (2001).
101 You, W., Wang, L., Wang, Q. & Yu, L. Synthesis and structure/property correlation of fully functionalized photorefractive polymers. *Macromolecules* **35**, 4636–4645 (2002).
102 You, W., Cao, S., Hou, Z. & Yu, L. Fully functionalized photorefractive polymer with infrared sensitivity based on novel chromophores. *Macromolecules* **36**, 7014–7019 (2003).
103 Hwang, J., Sohn, J. & Park, S. Y. Synthesis and structural effect of multifunctional photorefractive polymers containing monolithic chromophores. *Macromolecules* **36**, 7970–7976 (2003).
104 Gubler, U., He, M., Wright, D., Roh, Y., Twieg, Y. R. & Moerner, W. E. Monolithic photorefractive organic glasses with large coupling gain and strong beam fanning. *Adv. Mater.* **14**, 313–317 (2002).
105 He, M., Twieg, R. J., Gubler, U., Wright, D. & Moerner, W. E. Synthesis and photorefractive properties of multifunctional glasses. *Chem. Mater.* **15**, 1156–1164 (2003).
106 Bai, Y., Chen, X., Wan, X., Zhou, Q., Liu, H., Zhang, B. & Cong, Q. Influence of molecular weight on the photorefractivity of polymer/liquid crystal composites. *Appl. Phys. Lett.* **80**, 10–12 (2002).
107 Tsutsumi, N. & Kasaba, H. Effect of molecular weight of poly(N-vinyl carbazole) on photorefractive performances. *J. Appl. Phys.* **104**, 073102 (2008).
108 Däubler, T. K., Bittner, R., Meerholz, K., Cimrová, V. & Neher, D. Charge carrier photogeneration, trapping, and space-charge field formation in PVK-based photorefractive materials. *Phys. Rev. B* **61**, 13515–13527 (2000).
109 Schildkraut, J. S. & Buettner, A. V. Theory and simulation of the formation and erasure of space-charge gratings in photoconductive polymers. *J. Appl. Phys.* **72**, 1888–1893 (1992).
110 Däubler, T. K., Kulikovsky, L., Neher, D., Cimrová, V., Hummelen, J. C., Mecher, E., Bittner, R. & Meerholz, K. Photoconductivity and charge-carrier photogeneration in photorefractive polymers. *Proc. SPIE* **4462**, 206–216 (2002).
111 Cheben, P., Del Monte, F., Worsfold, D. J., Carlsson, D. J., Grover, C. P. & Mackenzie, J. D. A photorefractive originally modified silica glass with high optical gain. *Nature* **408**, 64–67 (2000).
112 Lee, J.-W., Mun, J., Yoon, C. S., Lee, K.-S. & Park, J.-K. Novel polymer composites with high optical gain based on pseudo-photorefraction. *Adv. Mater.* **14**, 144–147 (2002).
113 Gallego-Gómez, F., Del Monte, F. & Meerholz, K. Optical gain by a simple photoisomerization process. *Nat. Mater.* **7**, 490–497 (2008).
114 Zhang, L., Shi, J., Yang, Z., Huang, M., Chen, Z., Gong, Q. & Cao, S. Photorefractive properties of polyphosphazenes containing carbazole-based multifunctional chromphores. *Polymer* **49**, 2107–2114 (2008).
115 Nishide, J., Tanaka, A., Hirama, Y. & Sasabe, H. Non-electric field photorefractive effect using polymer composites. *Mol. Cryst. Liq. Cryst.* **491**, 217–222 (2008).
116 Tanaka, A., Nishide, J. & Sasabe, H. Asymmetric energy transfer in photorefractive polymer composites under non-electric field. *Mol. Cryst. Liq. Cryst.* **504**, 44–51 (2009).
117 Li, H., Termine, R., Angiolini, L., Giorgini, L., Mauriello, F. & Golemme, A. High T_g, nonpoled photorefractive polymers. *Chem. Mater.* **21**, 2403–2409 (2009).
118 Kawabe, Y., Fukuzawa, K., Uemura, T., Matsuura, K., Yoshikawa, T., Nishide, J. & Sasabe, H. Photoinduced grating formation in a polymer containing azo-carbazole dyes. *Appl. Opt.* **51**, 6653–6660 (2012).
119 Kawabe, Y., Yoshikawa, T., Tada, K., Fukuzawa, K. & Imai, T. Phase-shifted gratings in azo doped polymers and their analysis by coupled-wave theory. *Proc. SPIE* **8827**, 88270R-1–88270R-8 (2013)
120 Gabor, D. A new microscopic principle. *Nature* **161**, 777–778 (1948).
121 Toal, V. *Introduction to Holography* Ch. 6 (CRC Press, Boca Raton, IL, USA, 2012).
122 Tay, S., Blanche, P.-A., Voorakaranam, R., Tunç, A. V., Lin, W., Rokutanda, S., Gu, T., Flores, D., Wang, P., Li, G. St, Hilaire, P., Thomas, J., Norwood, R. A., Yamamoto, M. & Peyghambarian, N. An updatable holographic three dimensional display. *Nature* **451**, 694–698 (2008).
123 Blanche, P., Tay, S., Voorakaranam, R., Saint-Hilaire, P., Christenson, C., Gu, T., Lin, W., Flores, D., Wang, P., Yamamoto, M., Thomas, J., Norwood, R. A. & Peyghambarian, N. An updatable holographic display for 3D visualization. *J. Display Technol.* **4**, 424–430 (2008).
124 Blanche, P.-A., Bablumian, A., Voorakaranam, R., Christenson, C., Lin, W., Gu, T., Flores, D., Wang, P., Hsieh, W.-Y., Kathaperumal, M., Rachwal, B., Siddiqui, O., Thomas, J., Norwood, R. A., Yamamoto, M. & Peyghambarian, N. Holographic three-dimensional telepresence using large-area photorefractive polymer. *Nature* **468**, 80–83 (2010).
125 Lynn, B., Blanche, P.-A., Bablumian, A., Rankin, R., Voorakaranam, R., St. Hilaire, P., LaComb, L. Jr, Yamamoto, M. & Peyghambarian, N. Recent advancements in photorefractive holographic imaging. *J. Phys. Conf. Ser.* **415**, 012050 (2013).
126 Tsutsumi, N., Kinashi, K., Sakai, W., Nishide, J., Kawabe, Y. & Sasabe, H. Real-time three-dimensional holographic display using a monolithic organic compound dispersed film. *Opt. Mater. Express* **2**, 1003–1010 (2012). Research Highlight in *Nature Photonics* **6**, 636 (2012).
127 Tsutsumi, N., Kinashi, K., Tada, K., Fukuzawa, K. & Kawabe, Y. Fully updatable three-dimensional holographic stereogram display device based on organic monolithic compound. *Opt. Express* **21**, 19880–19884 (2013).
128 Tsutsumi, N., Kinashi, K., Ogo, K., Fukami, T., Yabuhara, Y., Kawabe, Y., Tada, K., Fukuzawa, K., Kawamoto, M., Sassa, T., Fujihara, T., Sasaki, T. & Naka, Y. Updatable holographic diffraction of monolithic carbazole-azobenzene compound in poly(methyl methacrylate) matrix. *J. Phys. Chem. C* **119**, 18567–18572 (2015).
129 Kinashi, K., Wang, Y., Nonomura, A., Tsujimura, S., Sakai, W. & Tsutsumi, N. Dynamic holographic images using poly(N-vinylcarbazole)-based photorefractive composites. *Polym. J.* **45**, 665–670 (2013).
130 Salvador, M., Prauzner, J., Köber, S., Meerholz, K., Turek, J. J., Jeong, K. & Nolte, D. D. Three-dimensional holographic imaging of living tissue using a highly sensitive photorefractive polymer device. *Optics Express* **17**, 11834–11849 (2009).
131 Parrish, J. A. New concepts in therapeutic photomedicine—photochemistry, optical targeting and the therapeutic window. *J. Invest. Dermatol.* **77**, 45–50 (1981).
132 Joo, W.-J, Kim, N.-J., Chun, H., Moon, I. K. & Kim, N. Polymeric photorefractive composite for holographic applications. *Polymer* **42**, 9863–9866 (2001).
133 Sasaki, T. & Naka, Y. Dynamic amplification of optical signals in photorefractive ferroelectric liquid crystals. *Mol. Cryst. Liq. Cryst.* **614**, 106–117 (2015).
134 Wortmann, R., Glania, C., Krämer, P., Lukaszuk, K., Matschiner, R., Twieg, R. J. & You, F. Highly transparent and birefringent chromophores for organic photorefractive materials. *Chem. Phys.* **245**, 107–120 (1999).

Naoto Tsutsumi studied chemistry at Kyoto University and he received his Doctoral degree of Engineering in 1985 from Kyoto University. He joined Kyoto Institute of Technology in 1984. He was also a visiting researcher at the National Institute of Standards and Technology (NIST), USA, in 1988. Since 1997 he is a full Professor at Kyoto Institute of Technology and he is a vice President at Kyoto Institute of Technology in 2015. He has also been a Director of Center for Instrumental Analysis since 2002. He received SPSJ Mitsubishi Chemical Award in 2012. His research interests are electro-optical properties of polymers and polymer composites, organic nonlinear optics, photorefractive polymers for display application, organic diode lasers, ferroelectric polymer device and micro-fabrication using two-photon excitation.